

**GEOPHYSICAL ANALYSIS OF QUATERNARY MARINE SEDIMENTARY
PROCESSES, BONAIRE, NETHERLANDS ANTILLES**

A Thesis

by

MARY KATHRYN BALES

Submitted to the Office of Graduate and Professional Studies of
Texas A&M University
in partial fulfillment of the requirements for the degree of

MASTER OF SCIENCE

Chair of Committee,	Robert Reece
Committee Members,	Juan Carlos Laya
	Adam Klaus
Head of Department,	Michael Pope

August 2016

Major Subject: Geophysics

Copyright 2016 Mary Kathryn Bales

ABSTRACT

The island of Bonaire is an isolated carbonate platform that is formed of Miocene to modern carbonate successions overlying a Cretaceous igneous basement. We show that the igneous basement of the island of Bonaire, Netherland Antilles controls the seafloor topography and subsequently governs the location of most of the carbonate deposits especially the Holocene coral reef and the downslope transport of sediment. Our analysis from this combined sedimentary study focuses on; 1) identifying the source of the islands main sediment supply, where sediment is derived from and quantifying the sediment budget; 2) evaluating the main sediment transport mechanisms throughout the system and indicating the most influential factor; 3) assessing sediment transport from the coast to the basin by identifying sediment pathways and their morphology; and 4) locating sediment accumulation zones in all areas of the offshore environment.

To archive our objectives, we acquired ~172 km of 2D multichannel seismic reflection profiles on the western side of Bonaire to evaluate the marine environment off the coast of this isolated carbonate platform. By the integration of previous studies, both geological and geophysical, in addition to an assessment of Quaternary marine sedimentary processes within the system, we focus on the slope processes including sediment production and distribution. Production from both terrigenous and marine sources as well as transport mechanisms including mass transport and gravity driven downslope movement are studied. This study highlights the importance of understanding the morphology of the antecedent substrate on which a carbonate environment is

produced and how the climate and environment of Bonaire play a large role in sediment transport throughout our local system. The sediment processes observed in our study reveal contributing factors to the persistent carbonate production offshore Bonaire throughout the Quaternary and provide a modern analogue for other isolated carbonate platforms.

ACKNOWLEDGEMENTS

Foremost, I would like to express my gratitude to my advisor, Bobby Reece for all of his support and encouragement throughout my time at Texas A&M. He provided me with guidance in every step of this journey from our time in the field, in the classroom, conducting research, and discussing future career paths. I am grateful to have had an advisor who made such a large impact on my academic success and on my life. To my committee members, Juan Carlos and Adam Klaus, thank you for your contributions and the time you dedicated to the success of the project. Thanks go to Steffen Saustrup and the Paradigm support team for numerous hours of software support.

To Jacob Bayer, I cannot begin to express how fortunate I feel to have been able to work side by side these last two years. I thank him for the countless hours studying for class, processing data, writing, but mostly for always picking up the phone and listening to anything I had to say. I owe a huge part of my success to our friendship, thank you for being my rock.

A sincere thank you to my parents, sister and brother-in-law, my boyfriend John and all of my top-tier friends for their continuous support from day one to being at my thesis defense two years later. I could not have done it without them. They encouraged me through hard classes, teaching my first lab, and reminded me everyday that I had the knowledge and ability to complete my research and be a successful geologist. I love each of you and could not have asked for a better support system.

TABLE OF CONTENTS

	Page
ABSTRACT.....	ii
ACKNOWLEDGEMENTS.....	iv
1. INTRODUCTION.....	1
1.1 Geologic Background.....	3
1.1.1 Climate, Physical Setting, and Sea Level History.....	4
1.1.2 Carbonate Deposition.....	5
1.1.3 Holocene Carbonate System.....	6
1.1.4 This Study.....	7
1.2 2D Marine Seismic Reflection Data.....	8
1.3 Methods: Processing and Interpretation.....	9
2. OBSERVATIONS AND INTERPRETATIONS.....	10
2.1 Vertical Resolution.....	10
2.2 Acoustic Energy.....	10
2.3 Seismic Observation of Sub-Seafloor Reflectors.....	11
2.4 Seafloor Topography.....	13
2.4.1 Near-Shore Undulating Topography.....	14
2.4.2 Central and South Regions.....	15
2.4.3 North Region.....	17
2.5 Seismic Observation of Reflector Packages.....	19
2.6 Modern Carbonate Factory.....	20
2.7 Mesophotic Zone Morphology.....	21
3. DISCUSSION.....	23
3.1 Tectonic and Sea Level Implications.....	23
3.2 Topographic Controls on Carbonate Growth and Sediment Production.....	25
3.2.1 Ridges and Valleys.....	26
3.2.2 Near-Shore Undulating Topography.....	27
3.3 Sediment Sources.....	28
3.3.1 Sediment from Marine Environment.....	29
3.3.2 Subaerial Surface Erosion.....	31
3.4 Controls on Offshore Sediment Distribution.....	33

3.4.1	Wave Energy and Current Influences.....	33
3.4.2	Topographic Influences and Sediment Pathways.....	34
3.4.3	Storm Events and Mass Transport.....	37
3.4.4	Sea Level Fluctuation Influences.....	41
3.5	Sediment Accumulation and Traps.....	41
3.5.1	Accumulation Within Modern Reef Areas.....	42
3.5.2	Catchment Basins and Troughs.....	43
4.	CONCLUSIONS.....	45
5.	SUMMARY AND IMPLICATIONS.....	47
	REFERENCES.....	49
	APPENDIX A.....	55
	APPENDIX B FIGURES.....	67

1. INTRODUCTION

The island of Bonaire is located roughly 60 miles off the north coast of Venezuela in the Caribbean Sea (Fig. 1.1). Along with Aruba and Curaçao, the islands make up a chain known as the ABC islands that are part of the Leeward Antilles Ridge, which is located within the tectonically complex South Caribbean Plate Boundary Zone (SCPBZ). Bonaire was initially formed by volcanism in the early Cretaceous and uplifted as a result of subduction of the Caribbean plate beneath the South American plate starting in the Oligocene (Gorney et al., 2007; Hippolyte and Mann, 2011) and is classified as an isolated carbonate platform (Read, 1985). The morphology and evolution of the island is influenced by glacio-eustatic sea level fluctuations, tectonic uplift and subsidence, and physical geographic factors (Alexander, 1961; Hippolyte and Mann, 2011; Sulaica, 2015).

Carbonate production has occurred around the island since the early Pleistocene (Bandoain and Murray, 1974; De Buissonje, 1974; Sulaica, 2015). Four Pleistocene limestone terraces are exposed on land and formed due to sea level and tectonic influences (Alexander, 1961; Sulaica, 2015). The semiarid climate, location in warm tropical waters, and protection from high wave energy on the leeward (west) side of the island makes Bonaire an ideal region for coral growth and governed carbonate production since the Pleistocene (Taylor and Alfaro, 2005; van Duyl, 1985). Modern carbonate growth is expressed as a double-fringing reef on the west side of Bonaire with over 44 coral species (Green, 2012; Keller, 2011).

Holocene sediment within the Bonaire carbonate system is derived from two main sources; 1) sediment from the modern reef, both biogenically produced and bioeroded (Hall, 1999; Perry et al., 2012) and 2) climatic agents producing onshore erosion and run-off (Muhs et al., 2012; van Duyl, 1985). Previous studies state that sediment is predominantly located in grooves within the shallow marine terrace, <15 m water depth (Goreal and Land, 1974; van Duyl, 1985), and in sediment chutes that carry sediment from the shallow fore-reef to the deep fore-reef (Bak, 1977; Hall, 1999).

This study will use and an integration of marine 2D seismic reflection profiles acquired off the west coast of Bonaire as well as an accumulation of previous land, dive, and geophysical studies to evaluate the Quaternary marine sediment system. We aim to answer question about the location and morphology of sediment pathways from the near to offshore environment, how the seafloor topography is affecting those pathways, and factors influencing sediment accumulation occurring within the system. Information about these sedimentary processes helps us define the factors that are contributing to this thriving reef environment that has limited sediment supply and is located in a semiarid climate, and provides a better understanding to analogous systems.

1.1 Geologic Background

The island originated due to submarine volcanism during the early Cretaceous. During the mid to late Cretaceous into the Cenozoic, tectonic interaction between the Caribbean plate and the South American plate caused subsidence and shallow angle, southward-directed subduction (Gorney et al., 2007; Hippolyte and Mann, 2011; Silver et al., 1975). The plate collision led to the development of an accretionary wedge as the sedimentary material from the Caribbean Plate underthrusts the South American plate (Kellogg, 1984; Levander et al., 2006). The tectonic activity from the plate motion resulted in a 600 km wide plate boundary zone (Fig. 1.1) known as the South Caribbean Plate Boundary Zone (SCPBZ) that spans from Northern Venezuela out to the Venezuelan Basin (Gorney et al., 2007; Silver et al., 1975). As the Caribbean plate moves at ~20 mm/yr to the east relative to South America, both compressional and extensional structures are created in this zone (Hippolyte and Mann, 2011; Pérez et al., 2001; Trenkamp et al., 2002).

The Leeward Antilles volcanic island arc was structurally uplifted along the plate boundary and in modern times is topographically expressed along the SCPBZ as the ABC islands. The island basement consists mainly of volcanic rock with structural deformation resulting from the accretion of the Leeward Antilles caused by the collision of the Caribbean and South American plate during the Cretaceous (Beets et al., 1977; Hippolyte and Mann, 2011). This formation is known as the Washikemba Formation and

ranges up to a few thousand meters thick with a composition consisting mainly of rhyolite and dacite (Beets et al., 1977).

1.1.1 Climate, Physical Geography, and Sea Level History

The climate of Bonaire is semiarid, receiving less than 60 cm of rain per year with a majority of that during the months of October through January (Taylor and Alfaro, 2005). Easterly trade winds constantly blow on the east side of the island at an average of ~ 7.2 m/s, while the west side is protected from strong wind speeds (Bak, 1977). This creates wave heights up to 3.5 m high on the windward side of the island and less than 1 m on the leeward side (Taylor and Alfaro, 2005; van Duyl, 1985). The current flow around the island is governed by the Caribbean Current that flows from the southeast around Bonaire at an average of less than 0.5 m/s (Gordon, 1967; Sandin et al., 2008). These typical values of wave heights, wind speed, and current flow are fairly constant year round and are only affected by large storms roughly every 4-5 years (Meyer et al., 2003). Storm occurrences that affect the island are sparse due to the location of the island being south of the Caribbean hurricane belt (Meyer et al., 2003).

Glacio-eustatic sea level fluctuations have greatly influenced the morphology of Bonaire. During the Pleistocene, sea level variations and tectonic uplift resulted in four carbonate terraces to form around the island (Fig. 1.2) (Escalona and Mann, 2011; Muhs et al., 2012; Sulaica, 2015). During interglacial periods carbonate systems were deposited and subsequently exposed during glacial periods and uplift (Fig. 1.3) (Muhs et

al., 2012). Following the Pleistocene, the Last Glacial Maximum (LGM) occurred resulting in the sea level around the Caribbean to be 121 ± 5 m below current sea level (Fairbanks, 1989). Since then sea level has been on a rise during the Holocene and studied locally on Bonaire by Engel et al. (2014) using mangroves and lagoonal sediment cores (Fig. 1.4)

1.1.2 Carbonate Deposition

Pijpers (1933) published some of the first stratigraphic descriptions of the carbonates on Bonaire. Since then authors including, Bandoain and Murray (1974), De Buissonje (1974), Hippolyte and Mann (2011), and Sulaica (2015) have developed a more complete story of the carbonate stratigraphy through outcrop and core studies on land. Among the first succession of carbonate deposits are the thin, ~30 m thick, deposit of the Cretaceous Maastrichtian Ricon limestone. These are overlain by the Soebi Blanco conglomerate that is derived from both the Ricon limestone and the underlying volcanics (Pijpers, 1933). During the Miocene and through the Pliocene carbonate deposition continued and is exposed on land today as the Seroe Domi Formation (De Buissonje, 1974). The Seroe Domi can be identified based on its high angle dip and outcrops on the northern portion of the island (Fig. 1.5).

Overlying the Seroe Domi is a sequence of Pleistocene carbonate terraces that are exposed throughout the island, on both the leeward and windward sides (Fig. 1.5). The terraces are a result of continuous deposition and subsequent erosion as tectonic

deformation and glacio-eustatic sea level changes. Alexander (1961) and Engel et al. (2010) have further classified terraces morphology on the ABC islands and related the unique characteristics of the terrace profiles to trade winds and wave patterns. Sulaica (2015) studied the four exposed terraces on Bonaire using thin sections made from hand samples and cores that also underwent XRD analysis. His results provided detailed facies descriptions of internal terrace strata and information regarding their paleogeographic evolution.

1.1.3 Holocene Carbonate System

Holocene Carbonate System around the island has been studied by numerous authors including Lucia (1968), Bak (1977), Hall (1999), Engel et al. (2010), Keller (2011), and Green (2012). The sediment supply for the island is mainly controlled by the climate and the modern reef. Onshore sediment studies in the southern portions of the island show sediment filling Pleistocene carbonate depressions. This strata has been studied utilizing outcrop data and cores and is classified as supratidal deposits during a relative sea level high (Lucia, 1968). Holocene sediment also appears in three alluvial sites and multiple bokas (lagoons) around the island. This sediment is currently separated from the open ocean by a 9 m high ridge of coral rubble and is interpreted to be deposition from flooding during large storm events and lagoonal deposits from a pre-existing high stand sea level (Engel et al., 2013b). Modern onshore processes generating

sediment are limited to minute volumes of sediment derived from erosion of the Pleistocene carbonates during rare high winds or heavy rainfalls.

Sedimentation offshore is derived from carbonate reef production and marine organisms. The reef on the west side of Bonaire is classified as a double fringing reef with the first reef at depths of 10-40 m and the second at depths from 75-115 m (Keller, 2011). The reef has over 44 different species and is comprised of hard coral, soft coral and algae, sponges, unlithified sediment, and coral rubble (Green, 2012; Keller, 2011). In the modern system multiple marine species including the *A. palmata* reef zone, *Porites Porites Montastrea* and benthic foraminifera, among others, act as a constant source of biogenic sediment supply (Hall, 1999). Sea organisms, such as urchins, and Clinoid sponges also account for current sediment production due to bioerosion processes (Hall, 1999). All together though, the island has a relatively low sediment budget compared to that of other modern carbonate environments (Bak et al., 2005; Madden et al., 2013). The lack of abundant sediment accumulation helps protect the reef from sediment suffocation allowing it to be one of the most flourishing modern reefs (Green, 2012).

1.1.4 This Study

This purpose of this study is to perform a geophysical analysis of the Quaternary marine sedimentary system on the leeward side of Bonaire, by utilizing 2D marine seismic reflection data collected by our research group, bathymetry and classification

maps of near shore environments (Keller, 2011), and multiple dive studies of the modern reef (Bak, 1977; Focke, 1978; Green, 2012; Hall, 1999; van Duyl, 1985). Specific questions addressed include: (1) How is the seafloor topography affecting carbonate production, reef growth and sedimentation? (2) What are the main sources of sediment around the island and does their distribution vary? (3) What are the effects of common environmental factors on sediment distribution around the island? (4) Is sediment being trapped within the system and if so where and why is accumulation occurring in these locations?

1.2 2D Marine Seismic Reflection Data

This investigation into the Quaternary sedimentary processes of the Bonaire carbonate system will utilize multichannel seismic (MCS) dataset acquired in November 2014. The survey includes ~172 km of 2D MCS data on the western coast of Bonaire (Fig. 1.6). The source used in the acquisition was a DuraSparker manufacturer by Applied Acoustics. The frequency used during acquisition ranged from 300 to 1200 Hz with a max power of 1200J. The data was recorded on a 144 m-long, 24 channel streamer with a channel spacing of 6.25m; each channel contained 4 hydrophones.

The shot spacing for the survey was at 6-second intervals with an average boat speed of 4 knots resulting in an ~12.35 m shot spacing and a maximum of six fold. The survey design included interconnected lines orientated in multiple directions to image carbonate growth patterns, sedimentation patterns, and seafloor topography.

1.3 Methods: Processing and Interpretation

The seismic dataset was processed using Paradigm processing software Echos. Beginning processing steps involved setting up the geometry to match our survey design and performing a coarse data quality check through each line to filter any bad channels or shots within the lines. Next a spectral frequency analysis was performed on each line in order to accurately perform a true amplitude recovery, automatic gain control, and bandpass filtering. These steps were followed by a deconvolution of the data signal, velocity analysis, and a normal moveout. Lastly, a stack, finite-difference time migration, and muting were to maximize image quality. Detailed processing steps are provided in the appendix.

After processing, interpretations were made of the seafloor, carbonate packages, sedimentation, and faults using 2D Canvas and Section in the Paradigm suite. The seafloor was gridded individually in the north, central, and south areas of data collection sites using the Kriging algorithm in Paradigm.

2. OBSERVATIONS AND INTERPRETATIONS

2.1 Vertical Resolution

Following the Rayleigh Criterion for vertical resolution, a reflective interface must be $\sim 1/4$ wavelength in thickness to discern between separate reflections (Sheriff, 1992). This value can be determined by knowing velocity of the material and frequency information of the geophysical source since the wavelength equals velocity divided by frequency (Sheriff, 1992). As mentioned above the frequency of the sparker signal ranges from 300 HZ to 1.2 kHz. Spectral analysis reveals a dominant frequency of ~ 600 Hz. We assume P-wave velocity values at the seafloor to be 1,800 m/s for marine sediments (Griffiths, 1981), 5,000 m/s for carboniferous limestone (Kahraman and Yeken, 2008), and 6,000 m/s for igneous rocks (Griffiths, 1981). With these assumed velocities this survey has vertical resolution values of ~ 0.75 m in sediment at the seafloor, ~ 2 m in carbonate rock, and ~ 2.5 m in igneous rock. Knowledge of these values allows different scale interpretations dependent upon rock type.

2.2 Acoustic Energy

In the majority of the 2D MCS dataset, the only seismic reflector is the seafloor. This is due to the high impedance contrast created from the acoustic energy traveling through the water column, at a velocity of 1,500 m/s and density of 1 g/cm^3 , and

immediately contacting the modern seafloor substrate, a hard rock surface comprised of carboniferous limestone and igneous rock (Griffiths, 1981; Soest et al., 2014).

Carboniferous limestone has a velocity of 5,000 m/s and a density of $\sim 2.4 \text{ g/cm}^3$ (Kahraman and Yeken, 2008) and igneous rocks have a velocity of 6,000 m/s and a density of $\sim 3.0 \text{ g/cm}^3$ (Griffiths, 1981). This significant difference between water properties and the properties of the hard rock substrate creates a large difference in the acoustic impedance which affects the reflection coefficient between the layers and subsequently the attenuation of the signal (Yilmaz, 2001). A majority of the acoustic energy bounces off the hard seafloor, back through the water column resulting in the reflection of a strong multiple throughout the data, and very little attenuation into the subsurface. This impedance contrast occurs from both the carbonate and igneous substrates making it nearly impossible to distinguish between the two rock types in our dataset.

2.3 Seismic Observation of Sub-Seafloor Reflectors

Although the seafloor in the study region has created a high impedance contrast between the water and the hard rock substrate, throughout the survey six of the 2D seismic profiles contain reflectors beneath the seafloor: lines 12, 18, 25, 31, 32, and 37 (Fig. 2.1). The buried reflectors are located near the seafloor at water depths ranging from 380 to 660 ms TWT, vary in length from 430 to 2,000 m and are concave up with varying degrees on concavity (Figs. 2.2 and 2.3). In each location coherent reflections

cannot be observed in the zone between the seafloor and this reflector. The maximum thickness of this zone ranges from ~40 to 60 ms. The sub-seafloor reflector acts as the base of this feature, that is bound by the seafloor and this reflector. The sub-seafloor reflectors can be sorted into groups based on their overall shape: 1) those located at the base of lens-shaped feature at the seafloor (Fig. 2.3d, e), and 2) reflectors that exhibit a hummocky or undulating pattern at the base of this feature (Fig. 2.3a-c, f). The reflectors at the base of the lens shaped features are laterally continuous, while the hummocky reflectors are laterally discontinuous (Figs. 2.2 and 2.3). The feature in line 32 has a unique characteristic from the other five lines; it is over 1,000 m longer than the other features observed in the subsurface and it creates a positive topographic relief on the slope (Fig. 2.4). The feature is lens shaped and bound at the top by the concave down, semi-discontinuous seafloor. The basal reflector of this feature is the sub-seafloor reflector, which is relatively flat and appears to have similar seismic characteristics of the surrounding seafloor (Fig. 2.4). The characteristics of this feature are unique and only observed in this one locality within the dataset however; it likely exists in other areas where we do not have coverage.

The feature in line 32, bound by the seafloor and the sub-seafloor reflector, occurs in deep water on a gently sloping seafloor and lacks internal structures. We interrupt this feature in line 32 to be a landslide where the sub-seafloor reflector is the base of the slide deposit. The process of sliding has been observed in the near-shore environment around Bonaire by divers (Hall, 1999; van Duyl, 1985), leading us to believe that this feature that we observe further offshore could be of similar nature.

Studies in the Great Bahama Bank (Principaud et al., 2015) and offshore Hawaii (Hampton et al., 2004) show features within high resolution seismic data that are bound by two coherent amplitude reflectors and that do not contain internal structures. Both studies interpret the features to be landslide deposits due to their seismic characteristics, which is significant since like Bonaire, they are isolated carbonate platforms with similar slope angles and environmental factors that can trigger gravity driven deposits.

On the remaining seismic profiles, the subsurface reflectors sit at shallower water depths, ~300 m. We interpret these as regression sheets due to their lens shape, lack of internal reflections, and location on the slope. Lens-shaped features that lack internal reflectors seen in high resolution seismic reflection profiles off Molokai, Hawaii are interpreted to be transgressive sheets (Fig. 2.5) (Barnhardt et al., 2005). This system is significant because it is similar to Bonaire in that they both geographically located in unstable sea level regimes and have been affected by fluctuations of over 100 m that has resulted in erosion and deposition to lowstand sea levels (Barnhardt et al., 2005; Muhs et al., 2012). Both the regression and transgression of the shoreline can cause the displacement of sediment and carbonate material to occur within the system, as the material is moved based on sea level fluctuations. This interpretation of the sub-seafloor reflectors being the base of sea level regression deposits is based solely on seismic reflection data; direct sampling of these features is required to ground truth the seismic interpretations.

2.4 Seafloor Topography

This section outlines the observations and interpretations made on the topography of the seafloor on the leeward (west) side of Bonaire. The bathymetry maps derived from the seismic seafloor horizon pick enable us to analyze the seafloor morphology (Fig. 1.6). From these bathymetry maps we observe that the north region (Fig. 1.6a) has a significantly steeper offshore seafloor topography, as apparent by the close spacing of the contour lines compared to that of the central and south regions (Fig. 1.6b, c) where the contour lines are spaced farther apart.

2.4.1 Near-Shore Undulating Topography

Undulating topographic depressions ranging from 60-400 m in width appear along the coastlines in the north and central regions of the survey (Figs. 2.6 and 2.7). These features are characterized by u-shaped dips in the topography. We classify these features as troughs. The troughs are wider than typical sediment channels in the Bonaire carbonate environment which range from a few meters in the reef (van Duyl, 1985) to a few tens of meters in water depths ~200 m deep (Keller, 2011). The troughs are surround by topographic highs with clear, high amplitude, continuous reflectors (Figs. 2.8 and 2.10). Together, the highs and lows create an undulating pattern in the topography near the coastline that is located basinward of the modern reef and is observed within our data ~180-300 m offshore (Figs 2.6, 2.7, and 2.8). We do not have the data density coverage to determine the full extent of these features however; we know they are confined to within 1 km of the coastline. We interpret this undulating

topography to be geomorphology remnant of lithified carbonate rock. Alternatively, the seafloor substrate in this location could be the igneous platform however if that were the case we believe we would observe this topographic pattern in other localities randomly offshore. This undulating topography is seen only in the near-shore environment leading us to believe that it is more representative of specific coastal development, most likely carbonate rock.

The near shore undulating topography cannot be observed in the southern region in the topographic grid. However, data coverage is sparse, and the closest strike seismic profile is ~1 km from the shoreline. The strike lines in the north and central regions demonstrate this pattern are within ~180 to 300 m of the shoreline (Fig 1.6). Therefore the trough features and undulating topography could also be present in the southern region but this area is not imaged in our dataset.

2.4.2 Central and South Regions

The seafloor topography extending farther offshore than the undulations described above forms elongated topographic highs and lows trending perpendicular to the western coastline in the central and south study regions (Fig. 2.6). Seafloor depths range from highs of ~90 ms TWT to depths over 1,200 ms TWT (Fig. 2.6). We observe five distinct elongated highs in the southern region and three in the central region that extended as far as 5 km from shore (Fig. 2.6). The data within our study does not show a

distinct basin drop off, leading us to believe that the full extent of the elongated topographic highs spans beyond our data coverage and continues farther offshore.

The elongated topographic highs are interpreted as igneous ridges with the ridge axis extending perpendicular offshore. Two linear igneous ridges outcrop on the east side of Bonaire and are oriented parallel to each other (Sulaica, 2015). These ridges have a maximum elevation of 180 m and 130 m above sea level and are not overlaid by carbonate rocks due to their subaerial exposure causing erosion of the carbonates (Sulaica, 2015). The observation of the igneous ridges on land is significant to the interpretation offshore because it allows us to make a correlation of the morphology from an outcropped studied feature to the morphology observed offshore. It is important to note the size of the ridges on land is relatively smaller than those observed offshore, however the morphology between the two is similar. We do not believe these ridge features are of carbonate origin due to their large size and offshore extent. Opposing the ridges, are topographic lows extending offshore and appear as valley like features with gradual decreasing depth toward the basin. Within our study these valleys reach depths of ~1,200 ms TWT and contain bowl-shaped topographic depression dispersed throughout the valley (Figs 2.6 and 2.9). We interpret the bowl-shaped topographic depressions to be small-scale catchment basins (Figs. 2.6 and 2.9). Similar morphologic features on the oceanic volcanic island of Hawaii, offshore of the Kilauea volcano, are interpreted as catchment basins (Fig. 2.11) (Smith et al., 1999). The morphology offshore the Kilauea volcano is similar to Bonaire in that both locations are volcanic platforms, with steep slope angles, and topographic lows dispersed throughout the slope.

2.4.3 North Region

The steeply dipping north also shows characteristics of an undulating seafloor near the shoreline (Fig. 2.7). Seismic profiles oriented in the dip direction, perpendicular to the northern coastline, all contain hump-like features within ~110 to 180 m water depth and within a few hundred meters of the coastline (Fig. 2.12). Down slope from this feature, the seismic profiles in Zone A dip steeply offshore with only a slight change in topography around 675 to 825 m and continue to water depths of 930 m (Fig. 2.7). Seismic profiles in Zone B of the north region contain a more variable topographic signature with irregular highs throughout the down-dip portion of Zone B (Fig. 2.7, purple dotted box). The profiles in Zone B show a local high topographic feature offshore with a maximum depth of ~600 m water (Fig. 2.7). Profiles in Zone B extend as far offshore as the profiles in Zone A and C, however the Zone B profiles never reach the deep water depths of the profiles in the surrounding zones. Several profiles within Zone B show steep dip angles before the high topographic feature and have a thicker base at the slope break that thins into the high, down-dip features (Fig. 2.13). Zone C has similar characteristics to that of Zone A, with a steeply dipping slope downslope the initial hump like feature and reaching seafloor depths of ~900 m. Zone C contains additional topographic variations farther offshore that are moderate in size compared to Zone B followed by a quickly drop in depth basin ward (Fig. 2.7).

We interpret the hump like feature observed in the dip profiles to be the modern deep fore-reef edge due to its proximity to the shoreline, shape, and depth. This is a

common morphological feature observed in ramped and isolated carbonate environments around the world (Grammer et al., 2001; Pomar, 2001). Following the fore-reef edge Zone A's steeply dipping topography is a result of the nature of the igneous basement in this region. We believe slope edge deposits from the modern reef could be spread along the igneous seafloor however no depositional facies are observed here. High amplitude seafloor reflectors on the slope edge are also observed in the offshore environment at the Great Barrier Reef in Australia where sediment dispersal was observed during geological studies but not resolved by seismic imaging (Hinestrosa et al., 2014). The slight change in topography seen in Zone A at depths ~900 to 1100 ms TWT does not have a clear morphology. This feature could be variations in the igneous formation or a debris slide from the reef. Due to higher wave energy in the north region of Bonaire and historic large-scale tsunami events (Engel et al., 2013a) it is assumed that carbonate material is ripped off the reef and transported basinward onto the igneous basement. The irregular topographic highs throughout Zone B (Fig. 2.7) are unknown features with two developmental theories. One theory is that the irregular pattern in the seafloor is the result of structural deformation. The SCPBZ has a complex tectonic history that has resulted in regional and local faulting and folding throughout this area (Escalona and Mann, 2011). A local anticline has been interpreted on the north end of Bonaire during a land study (Hippolyte and Mann, 2011) and offshore in a geophysical study of the Venezuelan Basin (Silver et al., 1975). This anticline could be the cause of the local topographic high in Zone B and subsequently caused structural deformation to occur, resulting in an irregular seafloor.

A second theory for the structure is a mass transport complex. With a relatively high dip angle and observations of a thick base of reflectors at the slope break, this zone shows evidence of sliding as seen in analogous environments around the world (Mangipudi et al., 2014). Following the slide feature, we interpret that the irregular topographic high is the result of the transport of large carbonate material down slope (Figs. 2.7 and 2.14). Principaud et al. (2015), discuss the transport of similar, large-scale carbonate features within the Great Bahama Bank. We interpret a wedge of coral debris or sediment to be trapped between the slope break and the topographically high feature. The seismic response within this wedge is chaotic and irregular in shape similar to that of rubble described by Grossman et al. (2006). The interpretation of the profiles in Zone C show a combination of features similar to Zones A and B profiles. Zone C has evidence of smaller scale mass transport, represented by irregularities in the seafloor topography however has slope angles compare to Zone A that quickly reach deep depths.

2.5 Seismic Observations of Reflector Packages

Reflector packages are present in two distinct locations throughout the survey; 1) in undulating topographic lows perpendicular to the leeward coastline (Fig 2.8) and 2) in catchment basins within valleys of the central and south study regions (Figs. 2.6 and 2.9). The packages of reflectors are thicker than the surrounding seafloor reflectors and range from 15 to 60 ms TWT thick (Figs. 2.8 and 2.9). Each package appears to contain

two to four, parallel to sub-parallel reflectors, some with lateral continuity (Fig. 2.10c), semi-continuous (Fig. 2.10b) and some laterally discontinuous (Fig. 2.10a).

We interpret the packages of reflectors to be confined sediment packages based on their seismic character and location in a topographic low. The reflector package characteristics are similar with that of topographic low deposits and channel deposits in other submarine carbonate systems (Fig. 2.15) (Faugeres et al., 1999; Grossman et al., 2006; Hineostrova et al., 2014). Grossman et al. (2006) shows that channel fill deposits consisting of thick unconsolidated carbonate sand and rubble offshore Oahu, Hawaii creates a seismic signature similar to our interpreted sedimentary packages.

Additionally, the depositional environment at this location in Bonaire is similar to that of Oahu, Hawaii, which is dominated by limestone and volcanic substrate and carbonate sediment is predominantly deposited on the leeward side of the island.

The reflector packages observed in the dip-oriented line also contain similarities to that of sediment fill and are located within catchment basins (Figs. 2.6 and 2.9). Like discussed in Chapter 2.4.2 the catchment basins are analogous to features seen offshore the Kilauea Hawaii volcano (Smith et al., 1999). The Kilauea seismic reflection data and the Bonaire seismic reflection data show similar seismic responses for sediment accumulation in these features. We interpret these features within our data to be catchment basins for downslope sediment movement based on this evidence.

2.6 Modern Carbonate Factory

At their most shallow depths, the summit of the ridge crests and the topographic highs along the coast line are shallow enough for modern carbonate production (Pomar, 2001). We assume carbonate production is occurring at these locations although direct core or hand sampling was not done offshore during this survey to verify carbonate build up. Dive surveys have been performed by several researchers including Bak (1977), Focke (1978), van Duyl (1985), and Green (2012) confirming modern reef development in this depth zone throughout the leeward side of the island. The seafloor topography at these shallow depths is highly irregular and has a discontinuous reflector (Fig. 2.16). Modern carbonate systems around the world including offshore Hawaii and the Florida Keys shows seismic characteristics similar to what we observe on Bonaire, with highly irregular seafloors within the photic zone and interpret these features to be modern reefal growth (Grossman et al., 2006; Lidz et al., 2003; Lidz et al., 1997). This is significant to the observations made on the seafloor topography of Bonaire to help identify regions of modern carbonate growth.

2.7 Mesophotic Zone Morphology

In addition to the seismic reflection profiles, we made observations on the bathymetry, backscatter, and still images acquired by Bryan Keller and a team of scientists from The University of Delaware and Virginia Institute of Marine Science (Keller, 2011). The data was collected in four zones on the west side of Bonaire from the shoreline to ~250 m offshore (Fig. 2.17). We use this seafloor data to extrapolate

observations from the seismic data closer to the shore where the seismic lines do not extend and to provide a more detailed interpretation in areas of data overlap.

Line 14 of the seismic data runs through the Marine Reserve study site in Zone 1. The sediment filled trough feature interpreted from the seismic data can be observed in Keller (2011) bathymetry map (Fig. 2.18a) and the classification map (Fig. 2.18b). The interpreted sandy bottom in the classification map spans ~600 m wide (Fig.2.18) and is interpreted to correspond to the trough feature from line14 (Fig. 2.8a). The observed depth shown in the bathymetry also correlates to the TWT seafloor measurement.

Small sand channels at depths greater than 200 m are observed in the swaths from Zone 1 and appear to widen basinward. Zone 4 also shows sand chutes up to 10 m deep (Keller, 2011). The highest percent of sandy bottom coverage is located within the channel or chute features and farther offshore in deeper depths past the reef, in gradually dipping areas. We observe small areas of sandy bottom extending laterally in front of the modern reefs in the classification maps. The coverage of the sandy bottom in front of the reef is minimal compared to the sediment coverage within the channel and chute features. Additionally the results from Keller (2011) Zone 2 images also show a high percentage of sandy bottom classification between Bonaire and Klein Bonaire.

3. DISCUSSION

3.1 Tectonic and Sea Level Implications

The island of Bonaire began as Cretaceous submarine volcanism on the transpressional South Caribbean Plate Boundary Zone between the Caribbean and South American plates (Fig. 1.1) (Hippolyte and Mann, 2011). It has since experienced tectonic uplift at a rate of ~ 5 cm/1000 years (Herweijer and Focke, 1978) as a result of shallow angle subduction of the Caribbean plate beneath the South American Plate (Gorney et al., 2007; Hippolyte and Mann, 2011) (Fig. 1.1). Tectonic uplift enabled the Cretaceous volcanics to reach depths shallow enough for carbonate production. Uplift, along with glacio-eustatic sea level fluctuations, resulted in the formation of a Miocene unit and of four Pleistocene carbonate terraces (Fig. 1.2) (Escalona and Mann, 2011; Muhs et al., 2012; Sulaica, 2015).

Sulaica (2015) hypothesized that since the subduction of the Caribbean plate occurs ~ 120 km north of Bonaire at a shallow angle, the northern part of the island is more strongly influenced by uplift and subsequently the southern portion of the island experiences subsidence. Subsidence rates, however, are not quantified. The driving mechanism behind why subsidence is occurring in the south is still only hypothesized however; several publications support this claim that subsidence is in fact occurring (Lucia, 1968; Scheffers et al., 2013; Soest et al., 2014; Sulaica, 2015). Sulaica (2015) observes that the first terrace is ~ 9 m above sea level in northern Bonaire and then

disappears in the south below a lagoon covered with modern deposits. During a study of Holocene sedimentation on southern Bonaire, Lucia (1968) describes sediment filling a Pleistocene depression. Although the Pleistocene unit was not dated in that study, it can be assumed that it is a depression within the first or second terrace because the other terrace formations are older and do not extend that far south (Fig. 3.1) (Sulaica, 2015). In addition, a submersible dive was performed in the central and southern regions on the leeward side of Bonaire to explore the deep water reefs off the coast (Soest et al., 2014). The study found the modern reef was growing in situ on steep limestone rock. These findings give evidence that the Pleistocene carbonates do in fact extend to the southern portion of the island and in the offshore regions where they are overlaid by modern sedimentation and reefal growth. This leaves the question remaining to what extents offshore do the Pleistocene terraces stretch and can that information help support the theory of subsidence for the southern portion of the island and possibly predict subsidence rates.

During the Last Glacial Maximum (LGM) sea level in the Caribbean was 121 ± 5 m below current sea level (Fairbanks, 1989). Since then sea level has been on the rise. Engel et al. (2014) constructed a local sea level curve for Bonaire that outlines the Holocene change in sea level (Fig. 1.4). If Bonaire has experienced ~ 5 cm/1000 years of uplift over the last 17,000 to 18,000 years (Herweijer and Focke, 1978), the current elevation of the island is ~ 0.85 - 0.90 m higher than during the LGM. We use the Engel et al. (2014) sea level curve and Herweijer and Focke (1978) uplift rates to infer an LGM paleo-shoreline around the north and central portions of the island on several of the

seismic lines. Since potential subsidence rates are not constrained in southern Bonaire, we only use sea level variation to construct the paleo-shoreline in the south.

This estimated LGM shoreline allows us to identify several localities that could have been subaerially exposed during the LGM.

3.2 Topographic Controls on Carbonate Growth and Sediment Production

Numerous studies have been conducted on the modern carbonate system off the leeward coast of Bonaire observing reef production, morphology, and factors controlling the near shore environment (Bak, 1977; Focke, 1978; Green, 2012; Keller, 2011; van Duyl, 1985). These studies are in a maximum of 300 m water depth with a majority of the research within the first 100 m. Details on slope angles are confined to within 200 m offshore and are constrained by specific dive locations (Focke, 1978). Bak (1977) discusses reef profiles on the leeward side of Bonaire where he observes a shallow submarine terrace ranging from 20 to 250 m wide followed by a drop off of 5-15 m deep into a steeper slope to depths up to 55 m and a second drop off between 50 and 80 m deep. Similar morphology is seen throughout the leeward side with differences of the fore-reef terrace in the north being narrower and ending more abruptly than in the south where the terraces are more expansive. Although these terraces are not sampled, and therefore cannot be directly related to the exposed terrace profiles on land, they show similar characteristics to the terraces on Bonaire described by Alexander (1961) and Sulaica (2015). These marine studies highlight the near shore topography but leave

unanswered questions about the topography farther offshore and how it relates to carbonate production and sedimentation transport and accumulation.

The bathymetry grids derived from the seismic reflection data and the profiles of each individual line allow us to address some of these unknowns and provide information about the offshore environment beyond the modern reef. Due to the Marine Protected Area (MPA) that surrounds the island we could not acquire data at depths shallower than 80 m and within 150 m of the coastline. As a result, we did not image the reef profiles outlined by Bak (1977) and Keller (2011) and our results cannot confirm the nature of the terrace profiles or the double reef feature with the seismic data. However, our survey continues offshore and reveals the topographic structure basinward of the (Bak, 1977) and (Keller, 2011) datasets.

Additionally, the survey provides a mean to update generalized bathymetry maps for the northwest and west side of Bonaire. Currently bathymetry contours are vague and generalized based on aerial photographs and satellite altimetry (Fig.3.2) (Engel et al., 2013a; Scheffers, 2005; Scheffers et al., 2013). The horizontal resolution of these images is several kilometers and does not accurately depict the seafloor topography.

3.2.1 Ridges and Valleys

The seafloor topography off the west side of Bonaire consists of irregular, ridges and valleys. This geomorphology is most likely controlled by the igneous basement Washikemba Formation. The ridges and valleys govern the location of modern reef

growth and guide sediment distribution offshore. In the central and south regions linear ridges orientated perpendicular to the shoreline create sediment pathways towards the basin between Bonaire and Curaçao (Fig. 2.6). Between each ridge valleys contain catchment basements that act as sediment traps.

The summits of the ridge crests and topographic highs that are within ~200 m depth of current sea level have the potential to be producing modern carbonates (Pomar, 2001). Although we are not imaging the main double reef structure observed by Keller (2011) because our reflection profiles do not extend close enough to shore, other carbonate species can prosper at greater depths. Deep-water sponges (Porifera) and other benthic species are studied at depths down to 248 m growing on moderately steep dipping slopes (Soest et al., 2014). These studies are all confined to near shore dive spots with the most distal survey extending offshore 1 km. This seismic study reveals several offshore, shallow locations atop linear ridges, for potential carbonate growth. To our knowledge divers, submersibles, or other geophysical studies have not evaluated these locations for modern growth. Within the study, we also observe that the low topographic nature of the valleys acts a primary mechanism to guide sediment flow offshore.

3.2.2 Near-Shore Undulating Topography

Irregular, undulating, sediment filled troughs are observed in the north and central study regions (Fig. 2.7). Seismic line 14 overlaps the deepest portion of the

swath data in Zone 1 from the Keller (2011) study (Fig. 2.17). Keller (2011) interprets the topographic lows to consist of sandy bottom and topographic highs to consist of coral rubble. Our seismic study has a vertical resolution of ~2 m in carbonate environments, making it possible to detect the accumulation of large carbonate rubble mounds. These rubble mounds are a plausible explanation for the irregular shape observed at the peaks of these topographic highs (Fig. 2.16). These features are not observed in lines farther offshore, implying that this system is limited to the near shore environment, within ~180-300 m of the coastline, with an uncertain basinward extent due to sparse data density. Similar coral rubble accumulations are observed on land on the west side of the island and classified as coral ridges along the coastline (Scheffers et al., 2013). These ridges are 2-3 m high and 40-80 m wide, were deposited due to wave events, and create a modern day barrier between the bokas and the open ocean (Scheffers et al., 2013). Keller (2011) seismic profiles and classification maps do not contain the resolution needed to map the extent of the coral rubble along the sea floor. We suggest that the same wave generated, environmental controls that developed the coral ridges now seen on land are occurring in the modern day marine environment.

3.3 Sediment Sources

In this section we will discuss controlling factors over the sediment budget on the west side of Bonaire. There are two main contributors to the source of sediment that is observed offshore Bonaire: biogenic and bioeroded sediment from the

marine environment and onshore surface erosion. Based on the evidence below we suggest that the marine environment is the dominant contributor to the sediment source of Bonaire.

3.3.1 Sediment from Marine Environment

The carbonate sediment production from a marine environment can be generated within three carbonate factories (or production systems): T (tropical), C (cool-water), and M (mud-mound) (Schlager, 2005). The dominant factory producing carbonate material in the modern day system around Bonaire is within the T factory meaning it is biotically controlled material that has precipitated from tropical autotrophic organisms and includes the modern, thriving, fringing, coral reef (Green, 2012; Schlager, 2005). This occurs within the top of the water column, generally with a depth window of ~100 m which coincides with typical water depths of the photic zone (zone of light saturation) (Schlager, 2005). As previously mentioned the modern fringing reef system on the west side of Bonaire, that is producing material within the T factory, has been greatly studied. Carbonate precipitates like micrite that are also biotically induced, and indicative of material from the M factory could be produced at greater depths around Bonaire (Schlager, 2005), however to our knowledge have not been studied.

Sediment production from the Bonaire marine environment is generated from two sources, sediment producers within the carbonate factories and marine driven erosion. The main component within the observed sediment offshore Bonaire is a sandy

rubble mixture (Bak, 1977). Autogenic processes including the health of the reef, wave patterns, water temperatures, sunlight, and the affect of bioeroders predominantly control sediment production offshore.

Biogenic carbonate sediment offshore Bonaire is predominantly produced within the T factory, which includes the coral reef (Focke, 1978; Hall, 1999; Schlager, 2005). The coral reef zone acts as a main contributor and is considered to be a “live” constant source of sediment for the modern system and includes, but is not limited to, *Montastraea*, *Agaricia*, *Porites*, *Stephanocoenia*, and *Palmata* genus (Green, 2012; Hall, 1999). In a census based sediment reef budget approach, Perry et al. (2012) estimates the net rate of carbonate production on the west side of Bonaire to be 9.52 to 2.30 kg CaCO₃ m⁻² year⁻¹. To our knowledge, the sediment budget in the marine environment, as a whole, is not quantified in any other study.

The fore-reef edge is dominated by intense bioerosion (biological substrate erosion) and subsequent sediment production (Hall, 1999; Perry et al., 2012). Studies from other modern carbonate environments have concluded that sediment produced as a result of bioerosion is along the same order of magnitude as reefal growth (Bergman et al., 2010). Clinoid sponges and parrotfish are the prime bioeroders in the Bonaire system (Hall, 1999; Perry et al., 2012). Clinoid sponges use chemical etchants to attack the coral resulting in losses in neighboring islands up to 1-23% of the bulk material (Hall, 1999). One study around Bonaire has shown that bioerosion from parrotfish accounts for 2.10 to 2.75 kg CaCO₃ m⁻² year⁻¹ (Perry et al., 2012). Sea urchins are also a strong contributor to bioerosion and have been measured in Curaçao to account for a total of 2.88 kg/m² per

year while feeding on both live and dead coral (Hall, 1999). While multiple studies on the exact sediment volume produced by each bioeroding agent at Bonaire has not been recorded and cannot be definitively stated, studies from the Maldives show that species like parrotfish account for greater than 85% of the sediment produced (Perry et al., 2015) and studies in the Bahamas equate roughly half of the sediment supply to sponges, echinoderms, bivalves, grazing fish gastropods, and microorganisms (Bergman et al., 2010). These organisms can cause destruction to the reef however are general observed feeding on dead coral substrate (Bergman et al., 2010; Hall, 1999).

The dead coral rubble additional provides a source of sediment as the rubble is abraded due to wave energy and slowly starts to break down (Soest et al., 2014). Hall (1999) estimates annual accumulation of sediment on the fore-reef zone to be 5.5 mm/year excluding sediment stored in reef framework, dissolved, or transported as suspended load. From the combined information provided during the geological studies, we infer that sediment production from the reef account for the majority of the overall supply to the system.

3.3.2 Subaerial Surface Erosion

Physical erosion generating sedimentation onshore Bonaire is less studied and popularly generalized based on allogenic processes including sea level fluctuations, producing erosional wave driven notches in the Pleistocene terraces, and regional climate variables.

The semiarid climate of Bonaire receives, on average, less than 60 cm of rain per year with the majority occurring from October to January (Taylor and Alfaro, 2005). Due to the easterly trade winds the leeward side of the island tends to be drier however during heavy showers and storm events water runs rapidly seaward in dried, narrow valleys, which serves to mobilize sediment (van Duyl, 1985). The trade winds also affect wave heights resulting in average heights of 2 to 3.5 m on the windward side and less than 1 m on the protected leeward side of the island (Taylor and Alfaro, 2005).

While wave energy can contribute to erosion, the leeward and windward coasts of Bonaire experience this process different. The high wave energy on the windward side generates substantially more sediment from erosion and is topographically expressed by sharp terrace cliffs. The more protected, the leeward (west), side is composed of rubble beaches and rocky shorelines. The rubble producing fringing reef on the leeward side prevents significant wave generated erosion and acts as a barrier for the onshore environment (Engel et al., 2013a).

Notches are observed on the leeward side of Bonaire and seen in both the 1st and 2nd terrace (Muhs et al., 2012; Sulaica, 2015). Although direct measurements estimating the amount of erosion occurring in these notches are not available, this autogenic process acts as a direct sediment supply to the marine environment. Additional small-scale, autogenic sediment supplies occur periodically during coastal development. Although these are a small influence in modern time, they can produce expansive amounts of sand over geologic intervals, causing damage to the active reef.

Through glacial-sea level changes landlocked bocas on the west side of the island could have been a strong contributor to the sediment supply offshore. Studies from Lucia (1968) and Engel et al. (2014) discuss extensive Holocene sediments in dried up carbonate depression on the low-lying south and in modern day bocas. These systems however are now isolated from the open ocean due to large coral rubble ridges and do not supply sediment offshore with the possible exception of during seasonal floods (Engel et al., 2010). Overall terrigenous sediment volumes from the island are not quantified and we speculate that their contribution to the offshore system is minimal.

3.4 Controls on Offshore Sediment Distribution

The transport of sediment on the leeward side of Bonaire is controlled by numerous factors including wave and current energy, topographic influences, tsunamis and storm events, and sea level fluctuation affects. The exact amount of sediment transport from each factor is difficult to quantify, however, evidence for each processes can be observed offshore within the seismic dataset and in previous studies.

3.4.1 Wave Energy and Current Influences

As mentioned above, typical wave heights on the leeward side of Bonaire are less than 1 m. Caribbean currents flow around Bonaire from the southeast and are generally slow, less than 0.5 m/s, on the leeward side (Gordon, 1967; Sandin et al.,

2008; Taylor and Alfaro, 2005). This low energy wave and slow current movement does not lead to large amounts of sediment transport. With the exception of the shallow *A. palmata* zone the modern reef is below the typical wave base. However, resuspension of sediments due to wave and current movement is common in reef environments and is observed on Bonaire (van Duyl, 1985). We believe that resuspension of sediment could account for the accumulation of sand along parts of the leeward shoreline but typical wave energy would not be sufficient enough to transport the larger pieces of coral rubble also seen along the shoreline.

3.4.2 Topographic Influences and Sediment Pathways

The topography that is controlling sediment dispersion can be organized in two parts; (1) by transport across the reef environment, including the fore-slope, and (2) transport beyond the reef, basinward (Fig. 3.3).

Transport of sediment across the reef and fore-reef slope, ~10-300 m offshore, has shaped the reef morphology and is observed topographically throughout the reef framework and appears across the entirety of the leeward coastal stretch. The near shore shallow reef terrace consists of a spur and groove system. The spurs are composed of coral reef and vary in width from 1-10 m and alternate with sediment grooves not exceeding 13 m wide (van Duyl, 1985). They are situated in 1 to 8 m water depth and are commonly formed from wave action (Goreal and Land, 1974; van Duyl, 1985). These narrow grooves act as the sediment pathway along the near shore and into the

mid- to low- terrace zone before they terminate (van Duyl, 1985). The morphology then transitions into wider sediment pathways identified as sediment chutes that carry sediment from the shallow fore-reef to the deep fore-reef slope (Fig. 3.3) (Bak, 1977; Hall, 1999; van Duyl, 1985). The sediment chutes range in width from 15-30 m wide and steep angle of the slope facilitates sediment evacuation from the reef (Hall, 1999). The bathymetry and backscatter data from Keller (2011) also observes sediment channels of this nature. Neither the geophysical data nor the dive data mentioned above discuss the thickness of the sediment within the chutes however, Hall (1999) states, as an order of magnitude calculation, that full distribution of the annual sediment production occurs throughout the sediment chutes within that year, resulting in the lack of in situ fore-reef sediment . Bak (1977), van Duyl (1985), and Hall (1999) all discuss the important nature of this sediment transport for the health of the reef and attribute this drainage of unconsolidated sediment downslope to be one of the strongest contributors to the modern thriving reef.

Once the sediment is transported past the modern reef system and into the deep fore-reef base, >300 m offshore, the large-scale topographic features observed in the seismic reflection data control transport (Fig. 3.3). In the north and central region the sediment first encounters the undulating trough features (Figs. 2.6 and 2.7). These topographic lows confine the sediment flow as it moves downslope. The sediment fill in the troughs ranges from 30-60 ms TWT thick. With an assumed sediment velocity of 1,800 m/sec this equals ~22-45 m. The state of lithification of the sediment packages observed in the troughs is unknown. It can be assumed that troughs with continuous to

semi continuous sediment reflectors (Fig. 2.10b and c) are in a stage of progressive lithification while troughs with a discontinuous sediment reflector (Fig. 2.10a) potentially are composed of a mixture of lithified and unlithofied sediment. The classification map from Marine Reserve Zone 1 (Fig. 2.18b) (Keller, 2011) classify the surface of these troughs to be sandy bottom allowing the interpretation to be made that an unconsolidated layer, of unknown thickness, covers the top of the troughs.

As the sediment continues to move offshore the valley features act as the pathway for sediment transport to the basin (Figs. 2.6 and 3.3). Due to the large-scale nature of these features we make the assumption that sediment dispersion occurs. We observe the occasional accumulation of sediment along the valleys in small catchment basins with the remaining sediment speculated to continue to move downslope. Sediment movement basinward in distal environments is typically a production of gravity driven, down-slope creep (Goreal and Land, 1974). Other islands in the Caribbean, Jamaica and the Virgin Islands, experience similar sediment transport from carbonate environments into the relatively shallow island basins like the basin between Curaçao and Bonaire which only reaches depths of 1,700 m (Bak, 1977; Chaytor and ten Brink, 2015; Goreal and Land, 1974).

The deepest sections of the valleys in the central and south regions and in zones A and C in the north region extend down to ~1,230 ms TWT, roughly 930 m water depth. The maximum depth between Bonaire and Curaçao is 1,700 m (Bak, 1977). The survey does not extend to the deepest sections of the basin between Bonaire and Curaçao

so we believe that deep basinward sediment transport continues past our survey until maximum depths are reached and the topography flattens.

Sediment is being transported from the coast to the deep basin through four distinct morphological features. First, the sediment is transported through grooves and sediment chutes in the near shore environment. Then sediment flows through the undulating trough features within ~180-300 m from the shoreline, finally to disperse within the igneous topographic valleys (Fig. 3.3).

3.4.3 Storm Events and Mass Transport

Fore-reef slopes on carbonate platforms that range from a 25-50° dip angle are prone to slope failures (Hall, 1999). The deep fore-reef slope of the Bonaire system reaches these angles and contain evidence of mass transport complexes. Slide scarps are documented in several dive locations around the island and have different morphologic features than slide scarps in terrestrial environments. The slide scarps around Bonaire are less arcuate and more tabular and leave a scarp with slope angles of ~40° (Hall, 1999). A slide that occurred in the central region left a scarp 20 m wide, 16 m tall, and 6 m deep, transporting a volume of ~1,900 m³ of carbonate material (Hall, 1999). The slide occurred at shallow water depths in unlithofied debris over a mobile carbonate mud transporting debris down to depths 50 m from the origin (Hall, 1999).

The sub-seafloor reflector in line 32 (Fig. 2.4) is interpreted to be the basal reflector of a mass transport or slide feature of carbonate material as well. The slide is at

the seafloor in 500 m water depth, is ~2 km long, and ~31 m thick. This slide is farther down slope and much larger in size than those described by Hall (1999). Additionally, the slide appears to be a more consolidated block-like feature, versus scattered debris. The difference in deposit geomorphology implies a difference in slide source material, and potentially difference in triggering factors.

Tropical storms impact Bonaire only every ~4-5 years due to location south of the Caribbean hurricane belt (Meyer et al., 2003). Storms have varying impacts on sediment transport on the leeward side of Bonaire; however generally do not disturb the coral reef in this location. On a relatively small scale, a storm will increase wave agitation on the reef, mobilizing sediment in the chutes and in the reef framework. Studies after Hurricane Lenny in 1999 showed sites where over 30 cm of sediment cover was removed from the reef system (Bries et al., 2004). At this scale the storm aided in sediment removal from the reef, but did not cause a significant amount of damage. Larger scale storms have a greater potential for reef destruction with their deeper-reaching wave base. This is one explanation for the interpreted carbonate slide from line 32. Suffocation of the reef can also occur if the storm causes a significant amount of surface erosion or brings sediment from offshore into the reef, however this is rare for Bonaire. Storms also have the ability to move sediment and reef material onshore from sand size particles, to coral rubble, and even large boulders (Engel et al., 2010; Engel et al., 2013b). This is most commonly the effect of category five storms or large tsunami events that create wave surges over that have the capability to transport boulder size material. Bonaire is vulnerable to the risk of tsunamis due to the complexity of the

tectonic regime it sits on (Engel et al., 2010). Onshore transport events are seen in the bokas around the island and in the form of boulders up to 70 m³ located on top of the 1st terrace (Engel et al., 2013a; Engel et al., 2013b). Isolated large blocks of this size are not observed offshore in the seismic data but a tsunami scale event could explain a peculiar topographic feature in the north study area.

Zone B of the north study area is observed to have a high topographic feature with an irregular morphology in the down-dip region (Fig. 2.7). Two possible interpretations are made for the development of this unique structure, one being that of a mass transport complex. Large-scale slope failures on steep carbonate slopes, like the slopes observed in northern Bonaire, are common and can occur due to numerous factors. Mass transport complexes of large size are typically triggered due to extreme storm event or slope failure due to sea level variations or tectonic movement (Hampton et al., 1996). The occurrence of all three of these triggers is common in Bonaire and could be responsible for the unknown structure. A large-scale carbonate submarine mass transport complex along the Great Bahama Bank consists of megablocks up to several thousands of meters in size and contains similar irregularly shaped carbonate mounds (Principaud et al., 2015). The slide scar for this complex is at an angle of 25° and has a scar up to 1 km (Principaud et al., 2015).

One major limiting factor to our interpretation of the feature is the composition. If the material was sampled and found to be composed of carbonate rock this interpretation would be highly plausible. The marine environment of Bonaire experiences multiple influences that could be factors in triggering mass transport, and

the irregular morphology of the feature resembles that of a reef like structure. If this is a mass transport complex, several questions remain: (1) why has the structure stopped on what appears to be the hinge axis of the local anticline (Hippolyte and Mann, 2011) and not continued under gravitational pull to the basin? (2) Can the slide scarp be identified and does it have similar characteristics of other carbonate slide scars on Bonaire? If this feature is a mass transport complex, the absence of a slide scarp could be contributed to timing and origin of the complex. Re-structuring of scarps is a common process in carbonate systems and observed in the near shore environment of Bonaire by (Hall, 1999). The Hall (1999) study evaluates the process of slide scars developing into sediment chutes over geologic time. If this mass transport complex occurred significantly early in the evolution of the island, the slide scarp could be reworked, not mimicking recent scarp morphologies. Another explanation for the absence of a slide scarp could be that the mass transport complex originated subaerially, was detached from an outcropped formation, and transported into the offshore environment.

It is important to recognize that the two main mass transports features that we observe in the data have different geomorphologic characteristics. The slide on line 32 appears to be a more consolidated mass that has uniformly slid down the shallow slope in the south region of the dataset. The hypothesized mass transport feature in the north is more irregular in nature, displaying characteristics of an unconsolidated debris slide on steep topography resulting in a topographic high. These results indicate that different influences and environments that contributed to the triggering mechanism for each mass transport occurrence.

3.4.4 Sea Level Fluctuation Influences

Sea level fluctuations have greatly influenced the morphology of Bonaire and played a large role on affected sediment movement both on and offshore. Quaternary shoreline transgression moved sediment onshore as seen in bokas (Engel et al., 2010) and carbonate depressions in the south (Lucia, 1968). Shoreline regression at the LGM shifted carbonate production a few hundred meters deeper resulting in lowstand deposits farther downslope. This lowstand shoreline would have also exposed marginal shelf areas leading to an increase of erosion and transport to the new sea level. We see evidence for this due to the subsurface reflectors throughout the data that has been interpreted to be regression sheets. The regression sheets are located at water depths on around ~ 400 m (Figs. 2.2 and 2.3). Since the regression sheets do not appear to be localized to one region, it can be suggested that the physical cause regression driven sediment deposits affected the whole system; supporting the sea level control on the origin of those deposits.

3.5 Sediment Accumulation and Traps

Sediment accumulation in the Bonaire modern isolated platform is low compared to typical carbonate systems where sediment depositional patterns and a stratigraphic record of the evolution of the system can be identified (Bak, 1977; Focke, 1978; Hall,

1999; Hampton et al., 2004; Playton et al., 2010). This depositional information typically shows sediment accumulation in numerous depositional patterns and is dependent on slope and margin morphology (Playton et al., 2010). With the nature of the offshore environment of Bonaire being that of an isolated carbonate platform with a steep antecedent seafloor, typical sediment accumulation or depositional patterns are not observed. Although other carbonate environments, like the Bahamas, are considered isolated a comparison in the slope morphology between that of the Bahamas and Bonaire is drastically different due to the high angle seafloor and narrow antecedent terrace formations of which the coral reef of Bonaire grows (Bergman et al., 2010; van Duyl, 1985). Additionally, Bonaire has developed morphologic features within the reef to aid in the movement of downslope sediment transport like the grooves and chutes, riding the reef of large sediment accumulation (Hall, 1999). The sediment that has accumulated offshore is seen moderately in the framework of the reef (Bak, 1977), in topographic lows including catchment basins and troughs, and between Bonaire and Klein Bonaire (Keller, 2011).

3.5.1 Accumulation Within Modern Reef Areas

The majority of sediment in the modern reef is confined to the groves and chute features that move sediment downslope (Bak, 1977; Hall, 1999). Thin layers of sediment become trapped within turf algae and other common plant species in the reef (Bak, 1977; Green, 2012). In the classification map of Marine Reserve Zone 1 (Fig. 2.18b) we

observe small, laterally-extending sandy bottom classification in front of each reef in the double reef feature. This sediment is most likely trapped in front of coral framework without sufficient energy to get moved through or around the reef. Coral abundance decreases downslope and the amount of sediment increases (Bak, 1977). Keller (2011) survey also shows a high coverage of sediment, ~50%, between Bonaire and Klein Bonaire. We interpret this sediment cover to be a result of Klein Bonaire acting as a barrier from the reef to the slope. Low wave energy between the two islands does not allowing for the same volume of transport to occur around Klein Bonaire and then down slope. Sediment thickness measurements in the near shore system do not exist and the seismic reflection profiles do not extend this far onshore, so the volume of sediment cover cannot be calculated.

3.5.2 Catchment Basins and Troughs

Sediment accumulation seen on the seismic data is in catchment basins and in trough features. The thickest accumulation of sediments is recorded in the troughs and ranges from ~22 to 45 m. As discussed in Chapter 3.4.2 the degree of lithification of these sediments is unknown but the trough features act as a mechanism for confining sediment as it moves farther offshore. Extending down the valleys, in the central and south regions, sediment is also observed in small-scale catchment basins that are represented by local topographic lows within the valleys (Figs. 2.6 and 2.9). These catchment basins act as the last trap or accumulation zone between the near shore and

the deep basin. The package of reflections indicates the presence of sediment in the catchment basins, which tends to be significantly less than in the troughs. This result is expected as the majority of the sediment is originating in the near shore environment, sediment dispersal will decrease distally from the shore. Additionally, sediments move downslope, which spread and disperse sediments resulting in thinning out sediment layers over the catchment basin and potentially continue into a downslope creep into the basin.

4. CONCLUSIONS

The seismic reflection profiles around the leeward side of Bonaire have provided the means to better understand local sedimentation processes from the near shore environment to deep slope basin. The main findings for this project include:

The Cretaceous submarine volcanism most likely controls the seafloor topography off the coast of Bonaire. The topography creates large ridges and valleys that we speculate continue beyond the extent of our data. The ridges are shallow enough to promote the growth of carbonate material at current sea level. The valleys act as a large-scale guide for sediment transport to the basin.

Undulating seafloor topography is present between the reef and deep valley/ridge features. The lows in the undulations are sediment-filled troughs and the highs show evidence for possible modern reefal growth or coral rubble ridges influenced by downslope processes, gravity, and perhaps ocean currents.

There are two main modes of sediment transport, gravity driven downslope movement and mass transport. The sediment typically moves within a four-stage sediment pathway starting with grooves and sediment chutes in the near shore environment and transitioning into larger scale troughs and valleys farther offshore. These pathways widen basinward and cause sediment dispersal to occur distally from the coast.

Due to the morphology of the slope offshore Bonaire sediment accumulation is low on the island and does not show evidence of typical carbonate slope deposition. Relatively small amounts of sediment accumulation do occur in thin sheets trapped within the modern reef system, in troughs, and in local small-scale catchment basements within the valleys. The thickest accumulation of sediment is prevalent in the troughs.

5. SUMMARY AND IMPLICATIONS

This study details the geological and environmental controls that affect the sedimentary processes on the island of Bonaire. We seismically observe how Quaternary sedimentary processes and Holocene reef morphology are influenced by the seafloor topography. The nature in which the island was formed lends to steeply dipping slopes on the west side of Bonaire that allow for a fringing reef to grow along the narrow, shallow coastline. Farther offshore ridges and valleys extending perpendicular off the coastline dominate the topography. The valleys act as sediment pathways from the reef to the deep-water basin and the ridge crests are within the photic zone, allowing for potential coral reef growth to occur. Understanding the topographic expression of the seafloor provides a full picture of the sedimentary pathways from the near shore to the deep-water basin and allows us to make implications for the location of carbonate growth in the Holocene environment and speculate on where these processes occurred during paleo-sea level environments.

The dry climate and limestone terrace formations hinder sub-aerial erosional processes and produce minimal terrigenous sediment that is transported offshore. The main sediment source for the island is derived from modern carbonate production. Sediment from the modern reef is produced biogenically, largely in the *A. palmata* zone, and bioeroded due to sea urchins and other marine species. Although the system reveals only one significant sediment source, this study shows an active sediment distribution

network, with accumulation of sediment within the modern reef, troughs, and catchment basins and transport out of the near shore system to the deep-water basin.

This study provides an example of how sediment is distributed in semiarid, low weather systems, and the influence that the offshore morphology has on this distribution. Additionally, it highlights that sediment pathways in the reef provide a means for downslope sediment movement, ridding the modern reef from large amounts of sediment accumulation. These sedimentary processes, and the climatic setting, outline key contributors to the healthy, thriving Holocene reef on Bonaire and to the significant carbonate production throughout the Pleistocene. The results from this study have direct implications for other, semiarid-arid carbonate producing environments that are limited in sediment supply. Key modern analogues include the Red Sea and other southern Caribbean islands. Understanding the sedimentary processes in similar systems can help account for the health and longevity of the living reef in these analogous environments.

REFERENCES

- Alexander, C. S., 1961, The Marine Terraces of Aruba, Bonaire, and Curacao, Netherland Antilles: *Annals of the Association of American Geographers*, v. 51, no. 1, p. 102-123.
- Bak, R. P. M., 1977, Coral reefs and their zonation in Netherland Antilles, *Studies in Geology* v. 4, p. 3-16.
- Bak, R. P. M., Nieuwland, G., and Meesters, E. H., 2005, Coral reef crisis in deep and shallow reefs: 30 years of constancy and change in reefs of Curacao and Bonaire: *Coral Reefs*, v. 24, no. 3, p. 475-479.
- Bandoain, C. A., and Murray, R. C., 1974, Pliocene-Pleistocene Carbonate Rocks of Bonaire, Netherland Antilles: *Geological Society of America Bulletin*, v. 85, p. 1243-1252.
- Barnhardt, W. A., Richmond, B. M., Grossman, E. E., and Hart, P., 2005, Possible modes of coral-reef development at Molokai, Hawaii, inferred from seismic-reflection profiling: *Geo-Marine Letters*, v. 25, no. 5, p. 315-323.
- Beets, D. J., Mac Gillavry, H. J., and Klaver, G., 1977, Guide to the field excursions on Curacao, Bonaire, and Aruba, Netherland Antilles, 8th Caribbean Geological Conference, Volume 2: Curacao, Netherland Antilles.
- Bergman, K. L., Westphal, H., Janson, X., Poiriez, A., and Eberli, G. P., 2010, Controlling Parameters on Facies Geometries of the Bahamas, an Isolated Carbonate Platform Environment, In *Carbonate Depositional Systems: Assessing Dimensions and Controlling Parameters: The Bahamas, Belize and the Persian/Arabian Gulf*, Springer Netherlands. p.5-80.
- Bries, J., Debrot, A., and Meyer, D., 2004, Damage to the leeward reefs of Curacao and Bonaire, Netherlands Antilles from a rare storm event: Hurricane Lenny, November 1999: *Coral Reefs*, v. 23, no. 2, p. 297-307.
- Chaytor, J. D., and ten Brink, U. S., 2015, Event sedimentation in low-latitude deep-water carbonate basins, Anegada passage, northeast Caribbean: *Basin Research*, v. 27, no. 3, p. 310-335.
- De Buissonje, P. H., 1974, Neogene and Quaternary geology of Aruba, Curaçao, and Bonaire [Ph.D. dissertation: Utrecht Natuurwetenschappelijke Studiekring.

- Engel, M., Bruckner, H., Furstenberg, S., Frenzel, P., Konopczak, A. M., Scheffers, A., Kelletat, D., May, S. M., Schabitz, F., and Daut, G., 2013a, A prehistoric tsunami induced long-lasting ecosystem changes on a semi-arid tropical island--the case of Boka Bartol (Bonaire, Leeward Antilles): *Naturwissenschaften*, v. 100, no. 1, p. 51-67.
- Engel, M., Brückner, H., Scheffers, A. M., May, S. M., and Kelletat, D. H., 2014, Holocene sea levels of Bonaire (Leeward Antilles) and tectonic implications: *Zeitschrift für Geomorphologie, Supplementary Issues*, v. 58, no. 1, p. 159-178.
- Engel, M., Brückner, H., Wennrich, V., Scheffers, A., Kelletat, D., Vött, A., Schäbitz, F., Daut, G., Willershäuser, T., and May, S. M., 2010, Coastal stratigraphies of eastern Bonaire (Netherlands Antilles): New insights into the palaeo-tsunami history of the southern Caribbean: *Sedimentary Geology*, v. 231, no. 1-2, p. 14-30.
- Engel, M., May, S. M., Frenzel, P., Scheffers, A. M., Kelletat, D. H., and Bruckner, H., 2013b, Holocene tsunamis in the southern Caribbean: Evidence from stratigraphic archives and the coarse-clast record, *Paleoseismology, Active Tectonics, and Archeoseismology: Aachen, Germany*, p. 1-4.
- Escalona, A., and Mann, P., 2011, Tectonics, basin subsidence mechanisms, and paleogeography of the Caribbean-South American plate boundary zone: *Marine and Petroleum Geology*, v. 28, no. 1, p. 8-39.
- Fairbanks, R. G., 1989, A 17,000-year glacio-eustatic sea level record: influence of glacial melting rates on the Younger Dryas event and deep-ocean circulation: *Nature*, v. 342, p. 637-642.
- Faugeres, J. C., Stow, D., Imbert, P., and Viana, A., 1999, Seismic features diagnostic of contourite drifts: *Marine Geology*, v. 162, p. 1-38.
- Focke, J. W., 1978, Holocene development of coral fringing reefs, Leeward off Curacao and Bonaire (Netherlands Antilles): *Marine Geology*, v. 28, p. 31-41.
- Gordon, A. L., 1967, Circulation of the Caribbean Sea: *Journal of Geophysical Research*, v. 72, no. 24, p. 6207-6223.
- Goreal, T. F., and Land, L. S., 1974, Fore-Reef Morphology and depositional processes, North Jamaica: *The Society of Economic Paleontologists and Mineralogists*, v. SP18, p. 77-89.
- Gorney, D., Escalona, A., Mann, P., Magnani, M. B., and Group, B. S., 2007, Chronology of Cenozoic tectonic events in western Venezuela and the Leeward

Antilles based on integration of offshore seismic reflection data and on-land geology: AAPG Bulletin, v. 91, no. 5, p. 653-684.

Grammer, G. M., Harris, P. M., and Eberli, G. P., 2001, Carbonat platforms: Exploration- and production- scale insight from modern analogs in the Bahamas: Leading Edge, p. 252-261.

Green, R. M., 2012, Analysis of Coral Reef Variation in Bonaire [Masters of Science: Indiana University, 86 p.

Griffiths, D. H., 1981, Applied geophysics for geologists and engineers: the elements of geophysical prospecting, Oxford, New York, Pergamon Press.

Grossman, E. E., Barnhardt, W. A., Hart, P., Richmond, B. M., and Field, M. E., 2006, Shelf stratigraphy and the influence of antecedent substrate on Holocene reef development, south Oahu, Hawaii: Marine Geology, v. 226, no. 1-2, p. 97-114.

Hall, D. B., 1999, The geomorphic evolution of slopes and sediment chutes on forereefs: Geomorphology, v. 27, p. 257-278.

Hampton, M. A., Blay, C. T., and Murray, C. J., 2004, Carbonate sediment deposits on the reef front around Oahu, Hawaii: Marine Georesources and Geotechnology, v. 22, p. 65-102.

Hampton, M. A., Lee, H. J., and Locat, J., 1996, Submarine landslides: Reviews of Geophysics, v. 34, no. 1, p. 33-59.

Herweijer, J. P., and Focke, J. W., 1978, Late Pleistocene depositional and denudational history of Aruba, Bonaire, and Curaçao (Netherland Antilles): Geologie en Mijnbouw, v. 57, p. 177-187.

Hinestrosa, G., Webster, J. M., Beaman, R. J., and Anderson, L. M., 2014, Seismic stratigraphy and development of the shelf-edge reefs of the Great Barrier Reef, Australia: Marine Geology, v. 353, p. 1-20.

Hippolyte, J.-C., and Mann, P., 2011, Neogene–Quaternary tectonic evolution of the Leeward Antilles islands (Aruba, Bonaire, Curaçao) from fault kinematic analysis: Marine and Petroleum Geology, v. 28, no. 1, p. 259-277.

Kahraman, S., and Yeken, T., 2008, Determination of physical properties of carbonate rocks from P-wave velocity: Bull Eng Geol Environment, v. 67, p. 277-281.

- Keller, B. M., 2011, Imaging the twilight zone: The morphology and distribution of mesophotic zone features, a case study from Bonaire, Dutch Caribbean [Master of Science: University of Delaware, 181 p.
- Kellogg, J. N., 1984, Cenozoic tectonic history of the Sierra de Perja, Venezuela-Colombia, and adjacent basins: Geological Society of American Memoir, v. 162, p. 239-261.
- Levander, A., Schmitz, M., Lallemand, H. G., Zelt, C. A., Sawyer, D. S., Magnani, M. B., Mann, P., Christeson, G. L., Wright, J. E., and Palvis, J. P., 2006, Evolution of the Southern Caribbean Plate Boundary: EOS, v. 87, no. 9, p. 97-104.
- Lidz, B. H., Reich, C. D., and Shinn, E. A., 2003, Regional Quaternary submarine geomorphology in the Florida Keys: GSA Bulletin, v. 115, no. 7, p. 845-866.
- Lidz, B. H., Shinn, E. A., Hine, A. C., and Locker, S. D., 1997, Contrasts within an Outlier-Reef System: Evidence for Differential Quaternary Evolution, South Florida Windward Margin, U.S.A: Journal of Coastal Research, v. 13, no. 3, p. 711-731.
- Lucia, F. J., 1968, Recent sediments and diagenesis of south bonaire, Netherlands Antilles: Journal of Sedimentary Petrology, v. 38, no. 3, p. 845-858.
- Madden, R. H. C., Wilson, M. E. J., and O'Shea, M., 2013, Modern fringing reef carbonates from equatorial SE Asia: An integrated environmental, sediment and satellite characterisation study: Marine Geology, v. 344, p. 163-185.
- Mangipudi, V. R., Goli, A., Desa, M., Tammiseti, R., and Dewangan, P., 2014, Synthesis of deep multichannel seismic and high resolution sparker data: Implications for the geological environment of the Krishna-Godavari offshore, Eastern Continental Margin of India: Marine and Petroleum Geology, v. 58, p. 339-355.
- Meyer, D., Bries, J., Greenstein, B., and Debrot, A., 2003, Preservation of in situ reef framework in regions of low hurricane frequency: Pleistocene of Curaçao and Bonaire, southern Caribbean: Lethaia, v. 36, no. 3, p. 273-285.
- Muhs, D. R., Pandolfi, J. M., Simmons, K. R., and Schumann, R. R., 2012, Sea-level history of past interglacial periods from uranium-series dating of corals, Curaçao, Leeward Antilles islands: Quaternary Research, v. 78, no. 2, p. 157-169.
- Pérez, O., Bilham, R., Bendick, R., Velandia, J. R., Hernandez, N., Moncayo, C., Hoyer, M., and Kozuch, M., 2001, Velocity field across the southern Caribbean plate

- boundary and estimates of Caribbean-South American plate motion using GPS geodesy 1994-2000: *Geophysical Research Letters*, v. 28, p. 2987-2990.
- Perry, C. T., Edinger, E. N., Kench, P. S., Murphy, G. N., Smithers, S. G., Steneck, R. S., and Mumby, P. J., 2012, Estimating rates of biologically driven coral reef framework production and erosion: a new census-based carbonate budget methodology and applications to the reefs of Bonaire: *Coral Reefs*, v. 31, no. 3, p. 853-868.
- Perry, C. T., Kench, P. S., O'Leary, M. J., Morgan, K. M., and Januchowski-Hartley, F., 2015, Linking reef ecology to island building: Parrotfish identified as major producers of island-building sediment in the Maldives: *Geology*, v. 43, no. 6, p. 503-506.
- Pijpers, P. J., 1933, *Geology and paleontology of Bonaire (N.W.I)* [Ph.D. dissertation: University of Utrecht.
- Playton, T., Janson, X., and Kerans, C., 2010, Carbonate Slopes, *Geological Association of Canada, Facies Models* 4.
- Pomar, L., 2001, Types of carbonate platforms: a genetic approach: *Basin Research*, v. 13, p. 313-334.
- Principaud, M., Mulder, T., Gillet, H., and Borgomano, J., 2015, Large-scale carbonate submarine mass-wasting along the northwestern slope of the Great Bahama Bank (Bahamas): Morphology, architecture, and mechanisms: *Sedimentary Geology*, v. 317, p. 27-42.
- Read, J. F., 1985, Carbonate platform facies models: *The American Association of Petroleum Geologist Bulletin*, v. 69, no. 1, p. 1-21.
- Sandin, S. A., Sampoya, E. M., and Vermeij, M. J. A., 2008, Coral reef fish community structure of Bonaire and Curaçao, Netherland Antilles: *Caribbean Journal of Science*, v. 44, no. 2, p. 137-144.
- Scheffers, A., 2005, Coastal response to extreme wave events-hurricanes and tsunamis on Bonaire: *Essener Geogr Arb*, v. 37.
- Scheffers, A. M., Engel, M., May, S. M., Scheffers, S. R., Joannes-Boyau, R., Hanssler, E., Kennedy, K., Kelletat, D., Bruckner, H., Vott, A., Schellmann, G., Schabitz, F., Radtke, U., Sommer, B., Willershauser, T., and Felis, T., 2013, Potential and limits of combining studies of coarse- and fine-grained sediments for the coastal event history of a Caribbean carbonate environment: *Geological Society, London, Special Publications*, v. 388, no. 1, p. 503-531.

- Schlager, W., 2005, Carbonate Sedimentology and Sequence Stratigraphy, Tulsa, Oklahoma, Society of Sedimentary Geology, Concepts in Sedimentology and Paleontology #8, 208 p.:
- Sheriff, R. E., 1992, Vertical and lateral seismic resolution and attenuation, Reservoir Geophysics, Tulsa, OK, Society of Exploration Geophysicists.
- Silver, E., Case, J., and Mac Gillavry, H. J., 1975, Geophysical study of the Venezuelan boarderland: Geological Society of American Bulletin, v. 86, p. 213-226.
- Smith, J. R., Malahoff, A., and Shor, A. N., 1999, Submarine geology of the Hilina slump and morpho-structural evolution of Kilauea volcano, Hawaii: Journal of volcanology and geothermal research, v. 94, p. 59-88.
- Soest, R. W., Meesters, E. H., and Becking, L. E., 2014, Deep-water sponges (Porifera) from Bonaire and Klein Curacao, Southern Caribbean: Zootaxa, v. 3878, no. 5, p. 401-443.
- Sulaica, J. L., 2015, Facies distribution and paleographic evolution of Neogene carbonates in Bonaire, Netherland Antilles [Master of Science: Texas A&M University.
- Taylor, M. A., and Alfaro, E. J., 2005, Central America and the Caribbean, Climate of, Encyclopedia of World of Climatology, Springer Netherlands, p. 183-189.
- Trenkamp, R., Kellogg, J. N., Freymueller, J. T., and Mora, H. P., 2002, Wide plate margin deformation, souther Central America and northwestern South America, CASA GPS observations: Journal of South American Earth Sciences, v. 15, p. 157-171.
- van Duyl, F. C., 1985, Atlas of the living reefs of Curacao and Bonaire (Netherland Antilles), Natuurwetenschappelijke Studiekring Voor Suriname en de Nederlandse Antillen, Utrecht, no. 117, p.1-91.
- Yilmaz, O., 2001, Seismic Data Analysis, Society of Exploration Geophysicists, Investigations in Geophysics.

APPENDIX A

Seismic reflection processing

This appendix is a summary of the workflow used to process the 2D multichannel seismic reflection data that was collected by our Texas A&M research team in 2014. Processing was performed using Paradigm's Echos software. The data was recorded in SEG-Y format and imported using a SEG-Y loader in Paradigm. Figure A.1 show the processing flow used for each line and table A.1 details file input and output information for each job. A brief summary of the final operations performed at each step are as followed (## indicate the place holder for the line name value, ex. 'line01'):

1. line##_1_geom.dat: Builds geometry tables including sample rate, data length, pattern specifications from streamer design, and shot location information from source. Figure A.2 and A.3 show raw data.
2. line##_2_geomapplystatic.dat: Reads SEG-Y into Echos from Paradigm database and applies specified geometry information. Amplitude analysis is performed in order to determine filtering needs (Fig. A.4). Results show a bandpass filter of 300-400-1200-1400 Hz is the best standard across the dataset. Additional notch filtering was needed for specific lines to increase image quality. Lastly a static correction of 104 ms shift is performed on out of plane shots.
3. line##_3_cdpsort.dat: Sorts the output from line##_2_geomapplystatic.dat job into CDP gathers.

4. line##_4_brutestack.dat: Creates a trace stack using the *normal* stacking algorithm in Echos with a scalar of 0.2. This stack was used to pick the water bottom (WB##) as a horizon to use for subsequent jobs including deconvolution and muting (Fig. A.8).
5. line##_5a_decon.dat: Applies a multichannel gapped predictive deconvolution. Before deconvolution, shot gathers were shifted to each respective WB## horizon pick using a static shift to hang the operation directly on the seafloor. Specifications for deconvolution include an operator length of 80 ms long, gap length of 1.5, and percentage of white noise 0.1% (Fig. A.5). After deconvolution is applied the static shift is removed and an additional bandpass filter is run.
6. line##_5b_sort.dat: Re-sorts the data output from line##_5a_decon.dat into CDP gathers and applies a spherical divergence (or gain) correction.
7. line##_6_veldef.dat: Job that opens an interactive velocity picking tool (Fig. A.6) for velocity analysis. Values were picked every 50 CDPs to get a coarse sample rate and accurate model (Fig. A.7).
8. line##_7_stack.dat: Applies an normal move out (NMO) correction, velocity function mute (mute##-for each respective line), and *normal* stacking algorithm to stack the traces.
9. line##_8_fxmig.dat: Performs a FX migration on the stack data using stored velocity picks, a lateral velocity smoothing of 200 and vertical velocity

smoothing of 100. An additional water bottom mute is applied after migration.

Final processed image after all jobs is shown in Figure A.9.

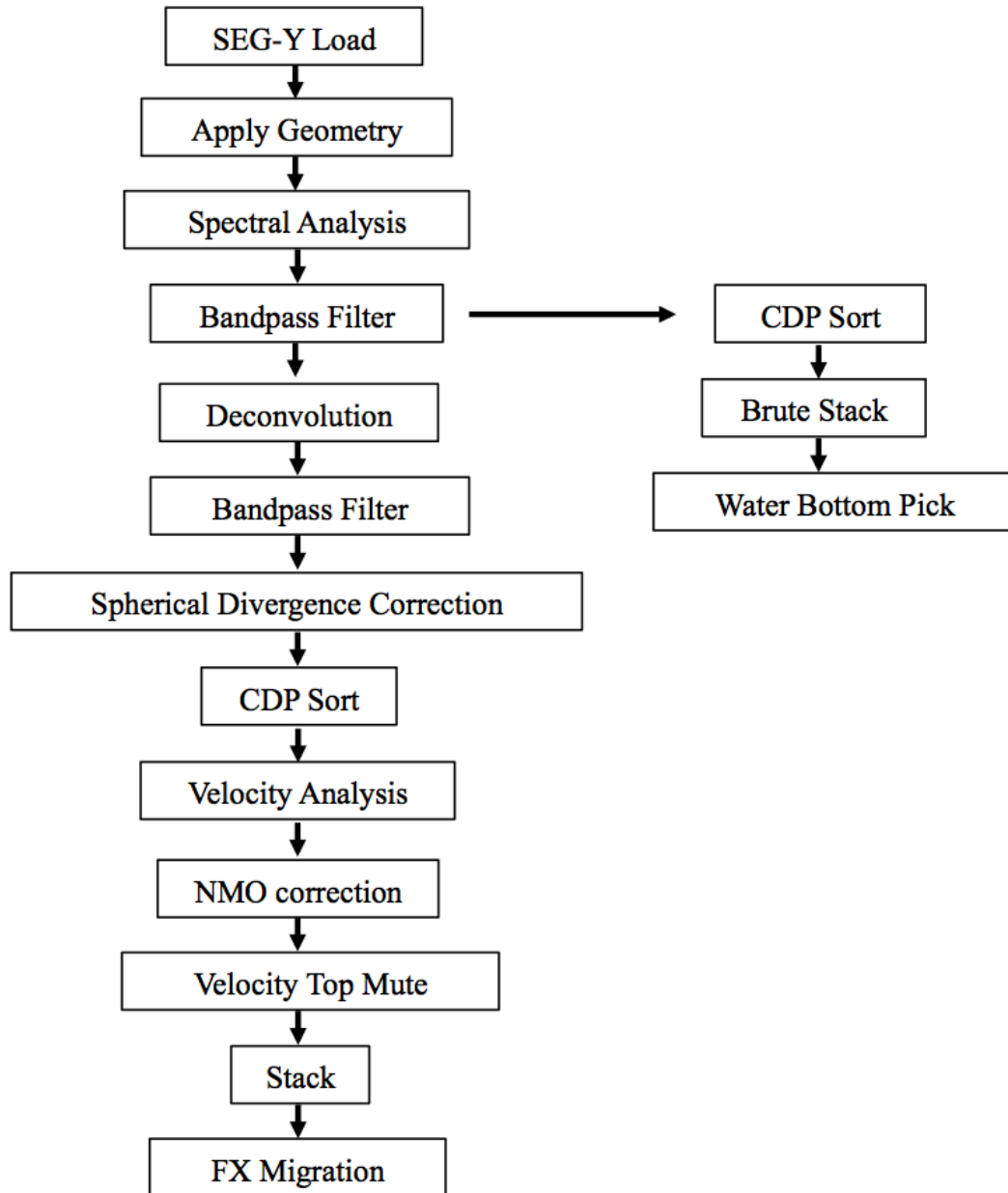


Figure A.1: Seismic reflection data processing workflow.

Job Name	Input File	Output File
line##_1_geom.dat	NA	NA
line##_2_geomapplystatic. dat	line##_new	line##_staticshots
line##_3_cdpsort.dat	line##_staticshots	line##_cdpsort
line##_4_brutestack.dat	line##_cdpsort	line##_brutestack
line##_5a_decon.dat	line##_staticshots	line##_shots_decon
line##_5b_sort.dat	line##_shots_decon	line##_cdps_decon
line##_6_veldef.dat	line##_cdps_decon	vel##. dat
line##_7_stack.dat	line##_cdps_decon	line##_stack_post_vel
line##_8_fxmig.dat	line##_stack_post_vel	line##_ migrated_stack_migfx

Table A.1: File input and output information for each job.

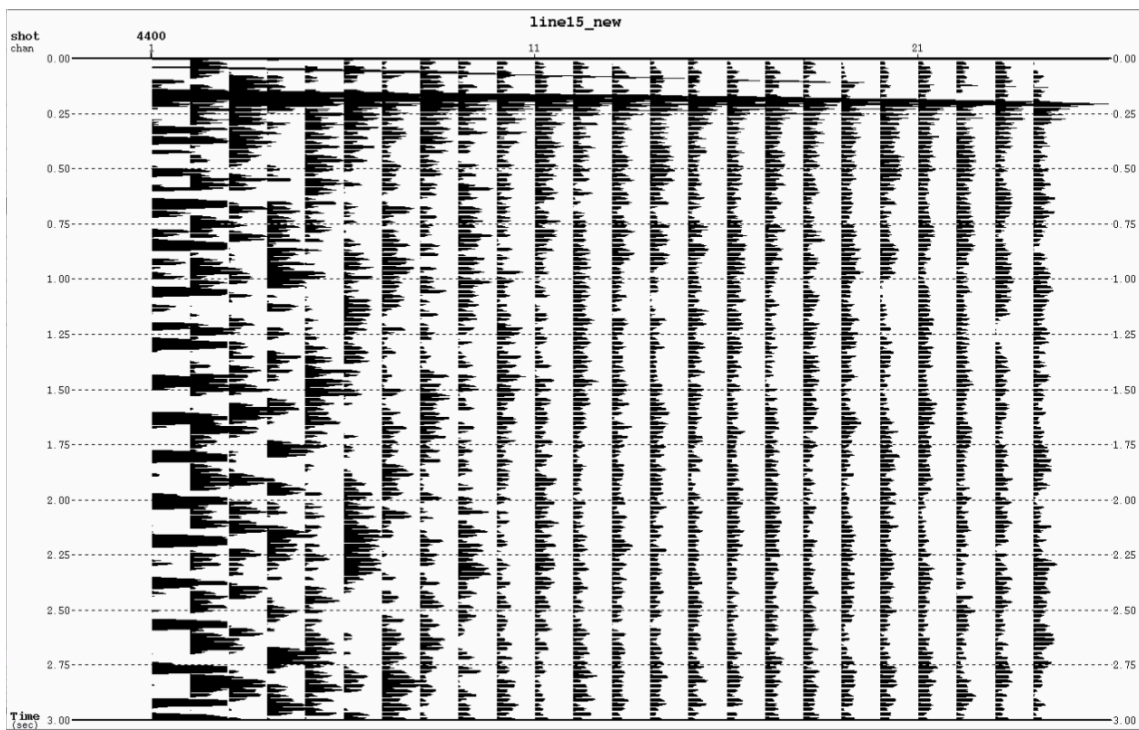


Figure A.2: Image of raw shot gathers prior to applying processing. Line15, shot 4400, channels 1-24.

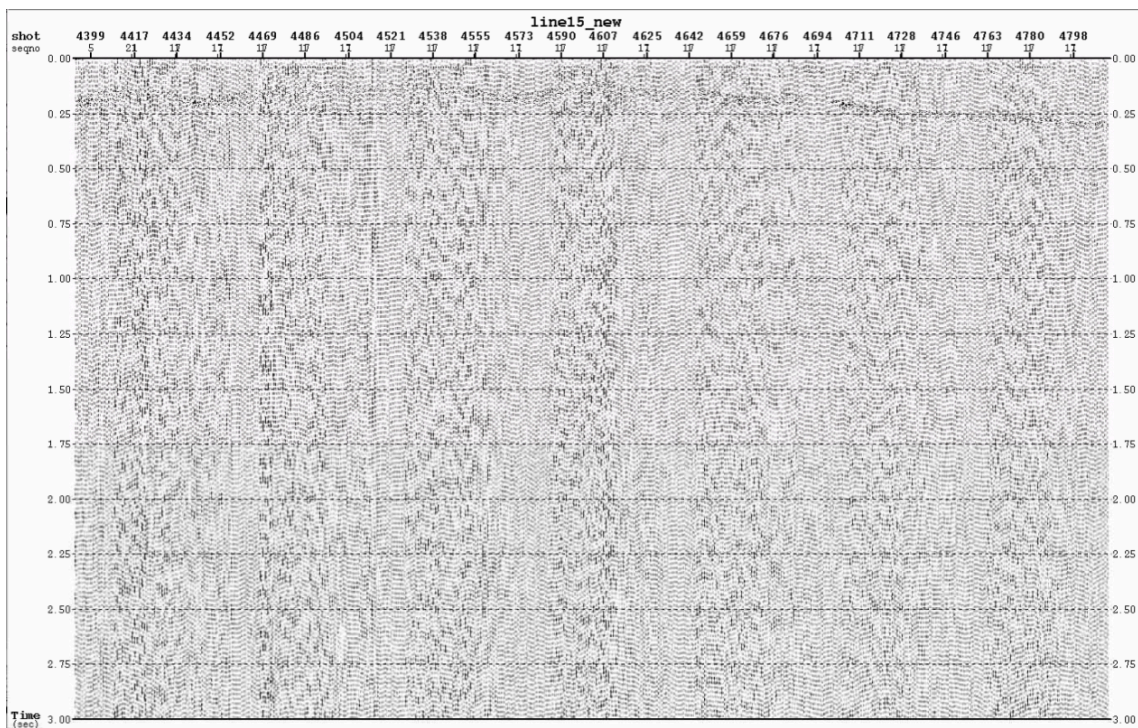


Figure A.3: Accumulation of all shots in line15. Raw shot gathers prior to applying processing.

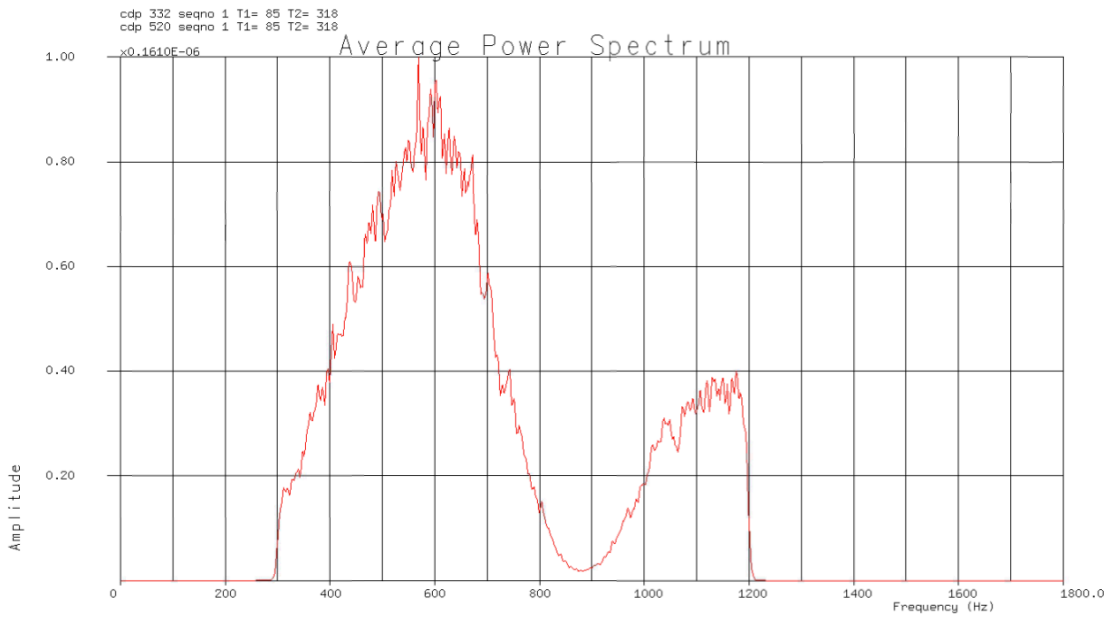
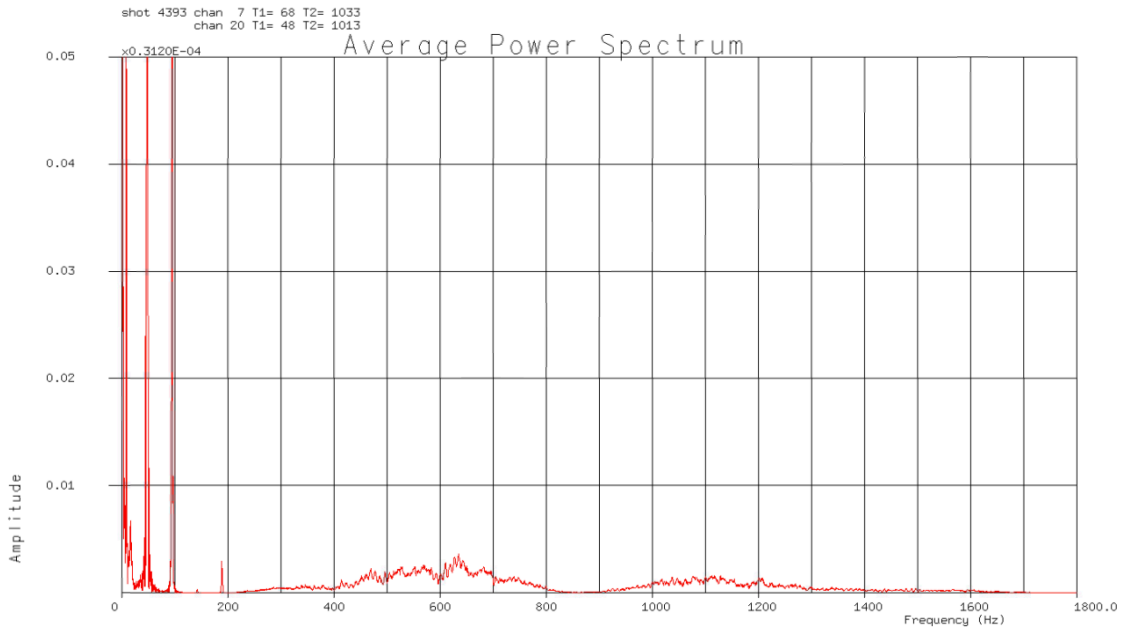


Figure A.4: Frequency analysis of raw shots from line 15 prior to processing (top).
Frequency analysis after bandpass filtering applied (bottom).

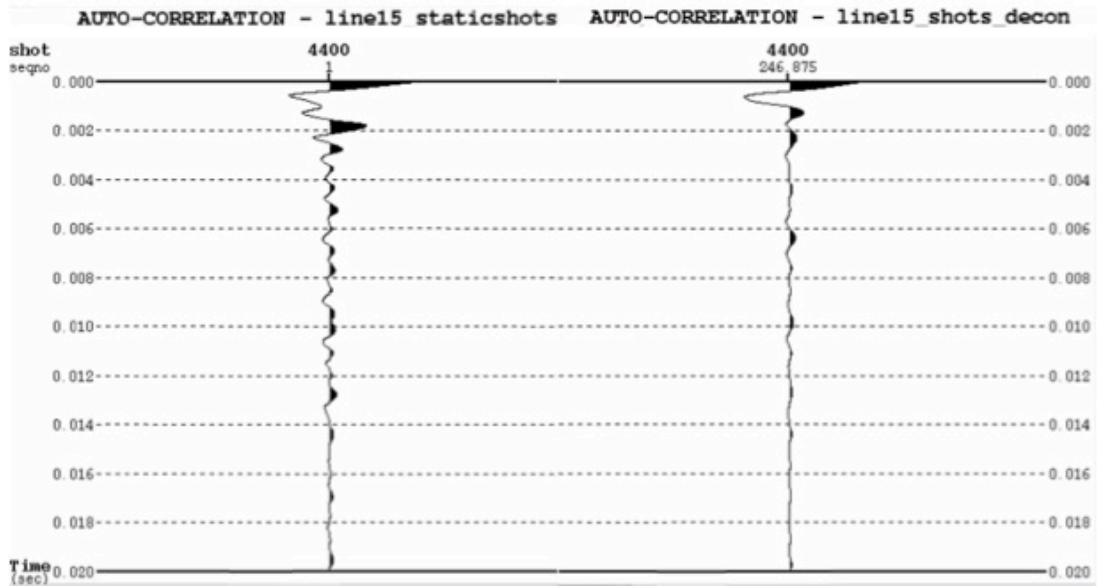


Figure A.5: Auto-correlation of 10 traces in one shot gather; before (left) and right (after) deconvolution.

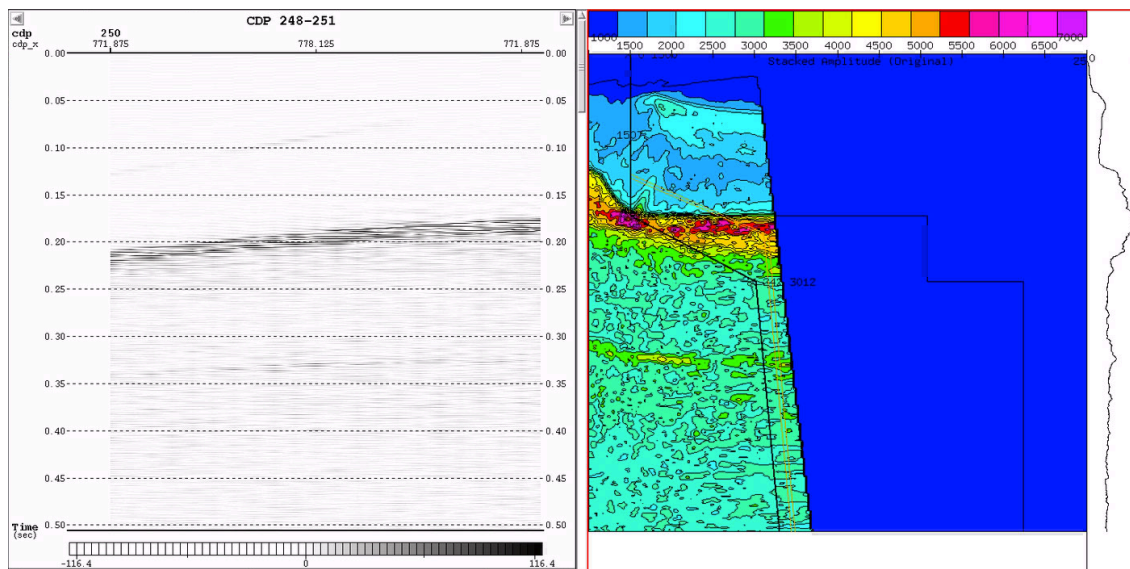


Figure A.6: Interactive velocity analysis window of Echos processing software zoomed into area of interest on line 15. Variable density image of stacked supergather of four CMPs (left). Coherence plot of seismic velocities with picked values (right).

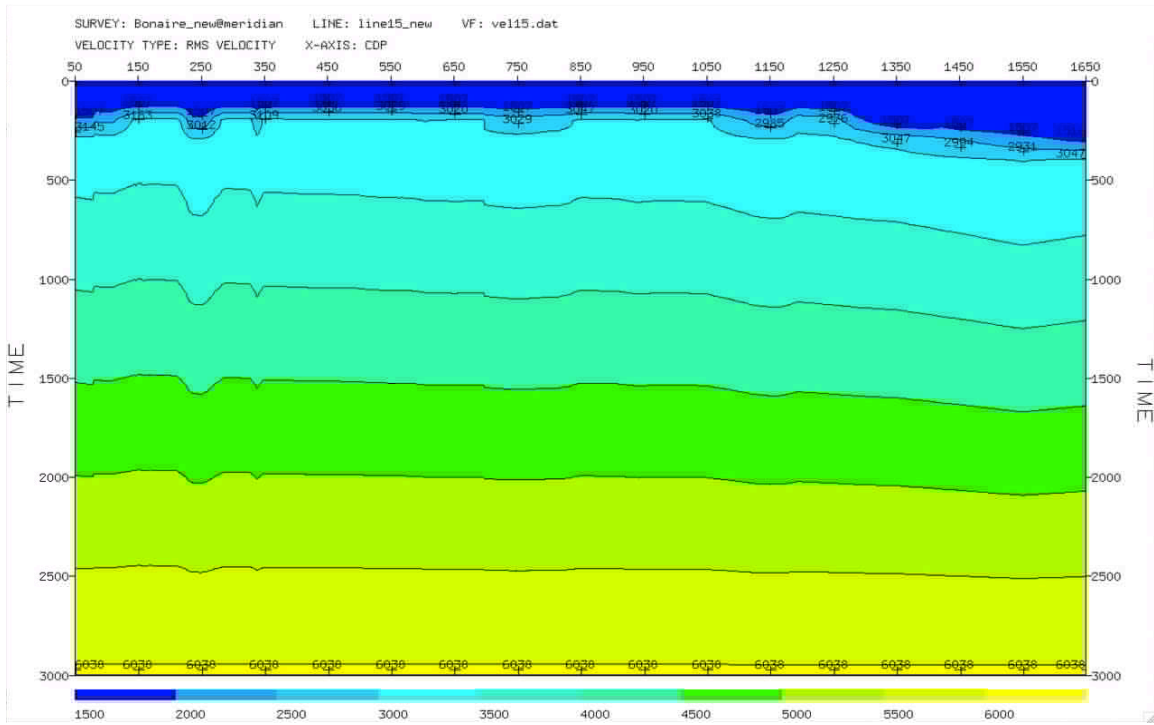


Figure A.7: Root mean square velocity model of line 15.

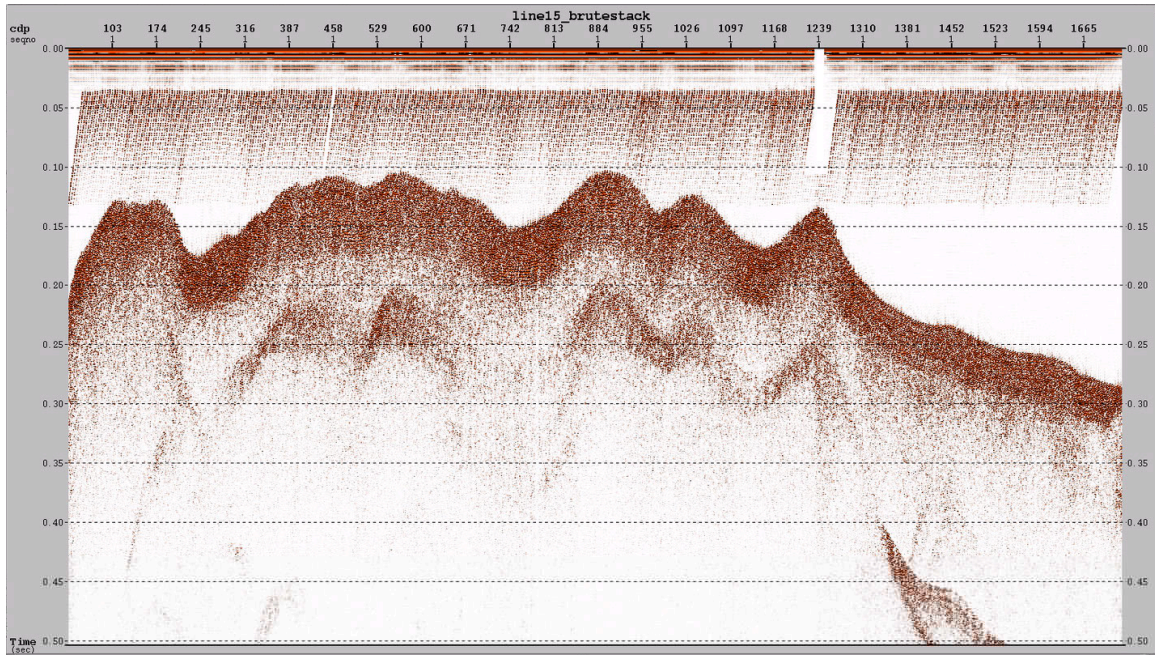


Figure A.8: Brute stack of line 15 with bandpass filter and prior to any further processing. Vertical exaggeration ~4:1

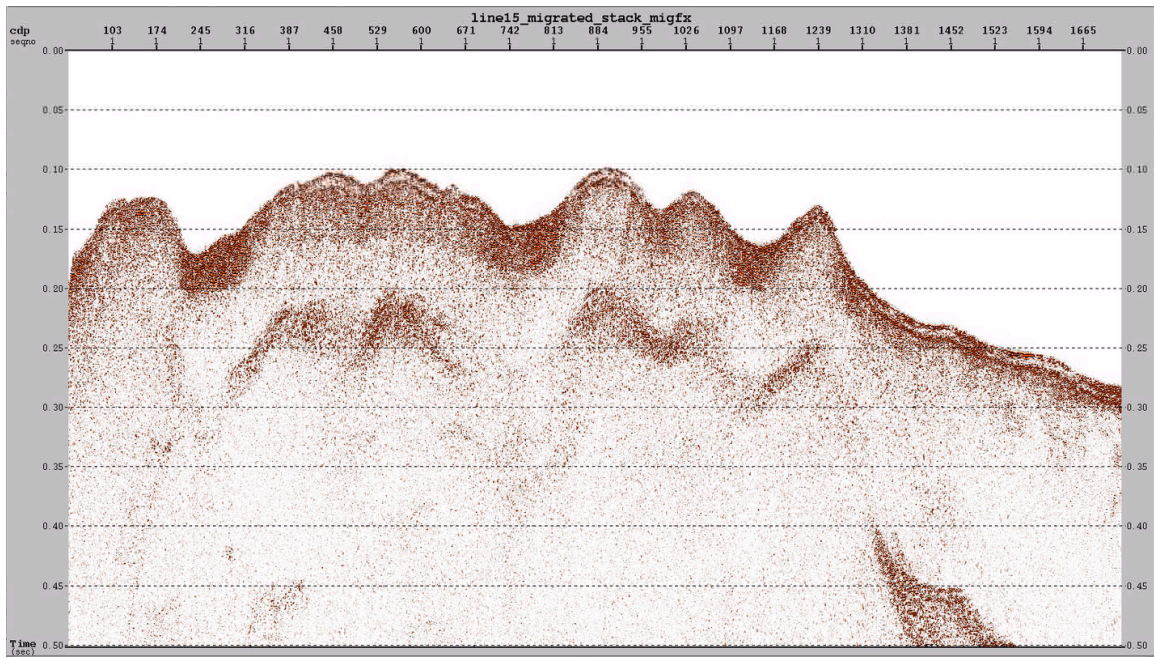


Figure A.9: Stack of line 15 with final processing steps (NMO, deconvolution, stack, mute, and migration). Vertical exaggeration ~4:1

APPENDIX B

FIGURES

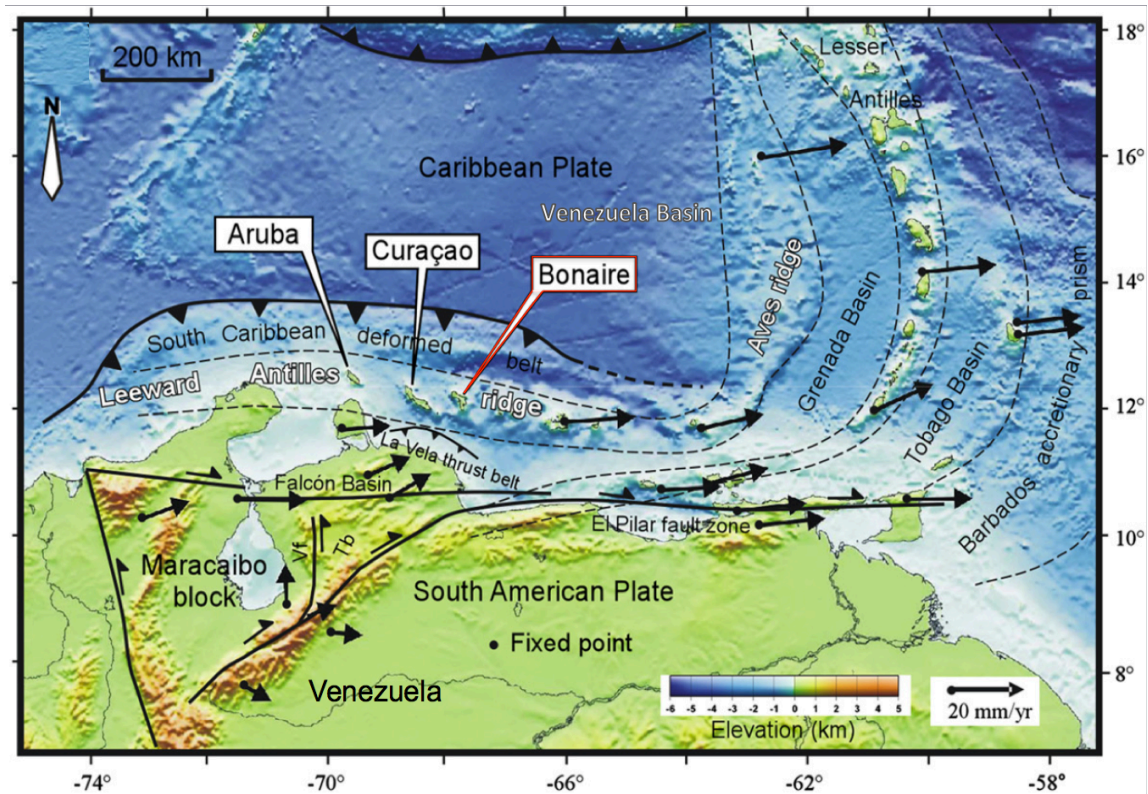


Figure 1.1: Tectonic setting of Bonaire, Leeward Antilles Ridge. Situated on the South Caribbean Plate Boundary Zone. Plate motion represented by GPS vector (black arrows) and tectonic provinces are separated by black dashed lines. Modified from Hippolyte and Mann (2011).

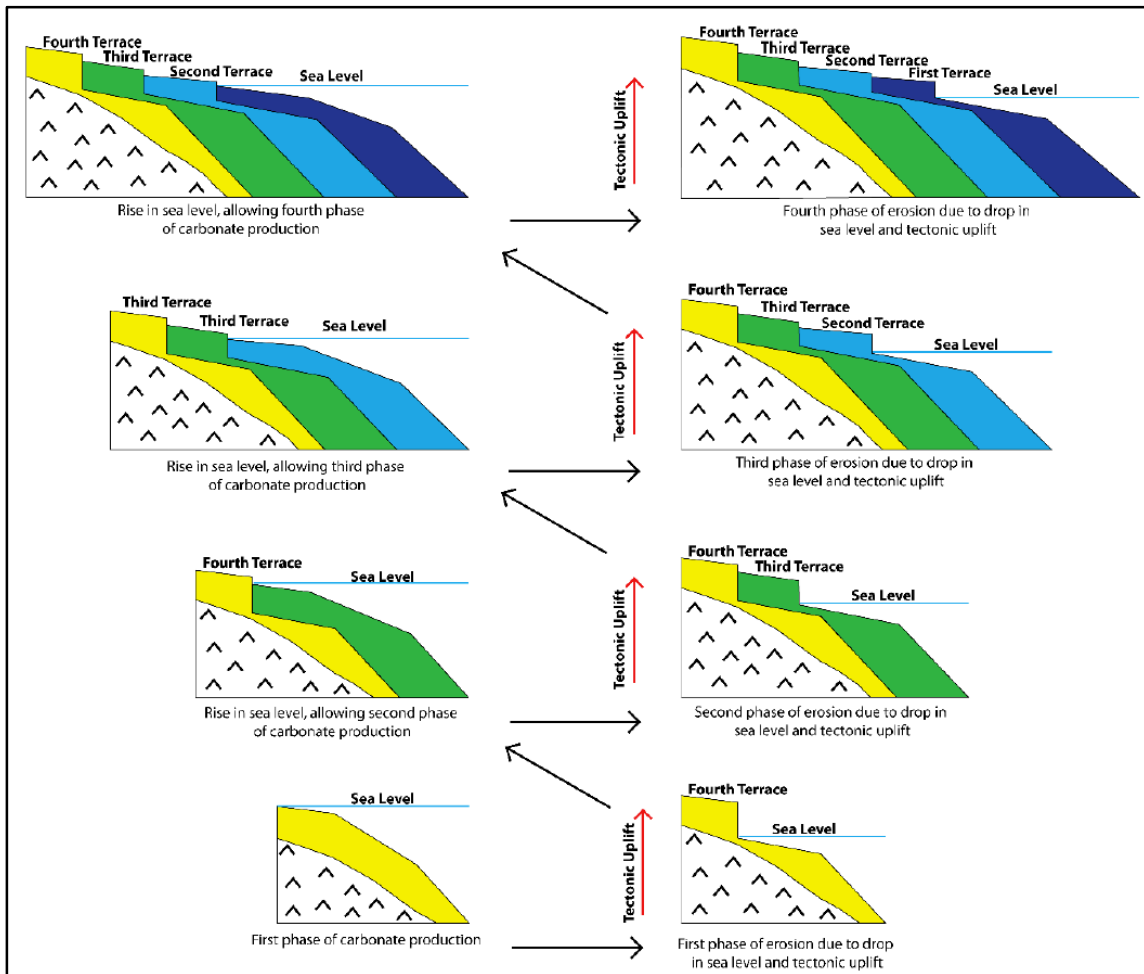


Figure 1.2: Terrace evolutionary model demonstrating growth with respect to sea level and tectonic influences on the eastern side of Bonaire. Each color represents a different carbonate terrace package while the Cretaceous igneous basement is in white and black (Sulaica, 2015).

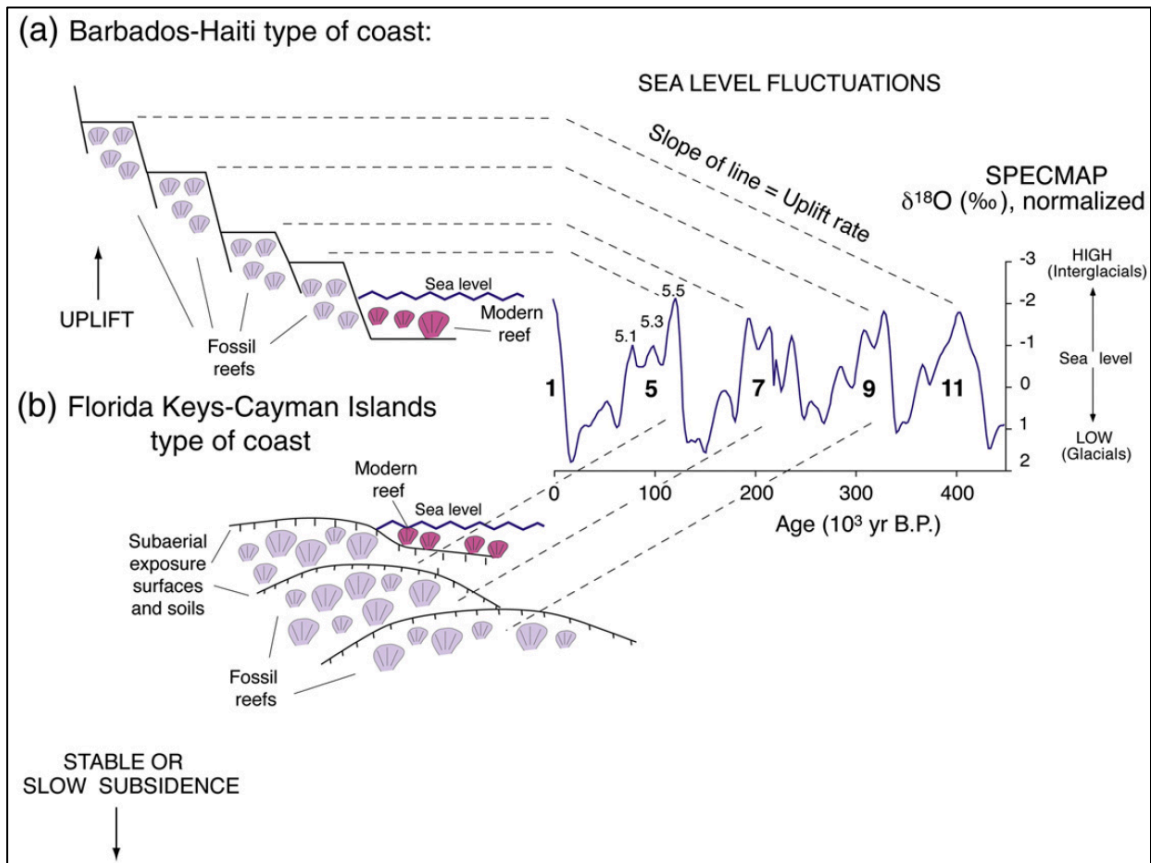


Figure 1.3: Pleistocene sea level curve relating interglacial periods and tectonic uplift to carbonate terrace formations. (a) Analogue to terrace formation on Bonaire (Muhs et al. 2012).

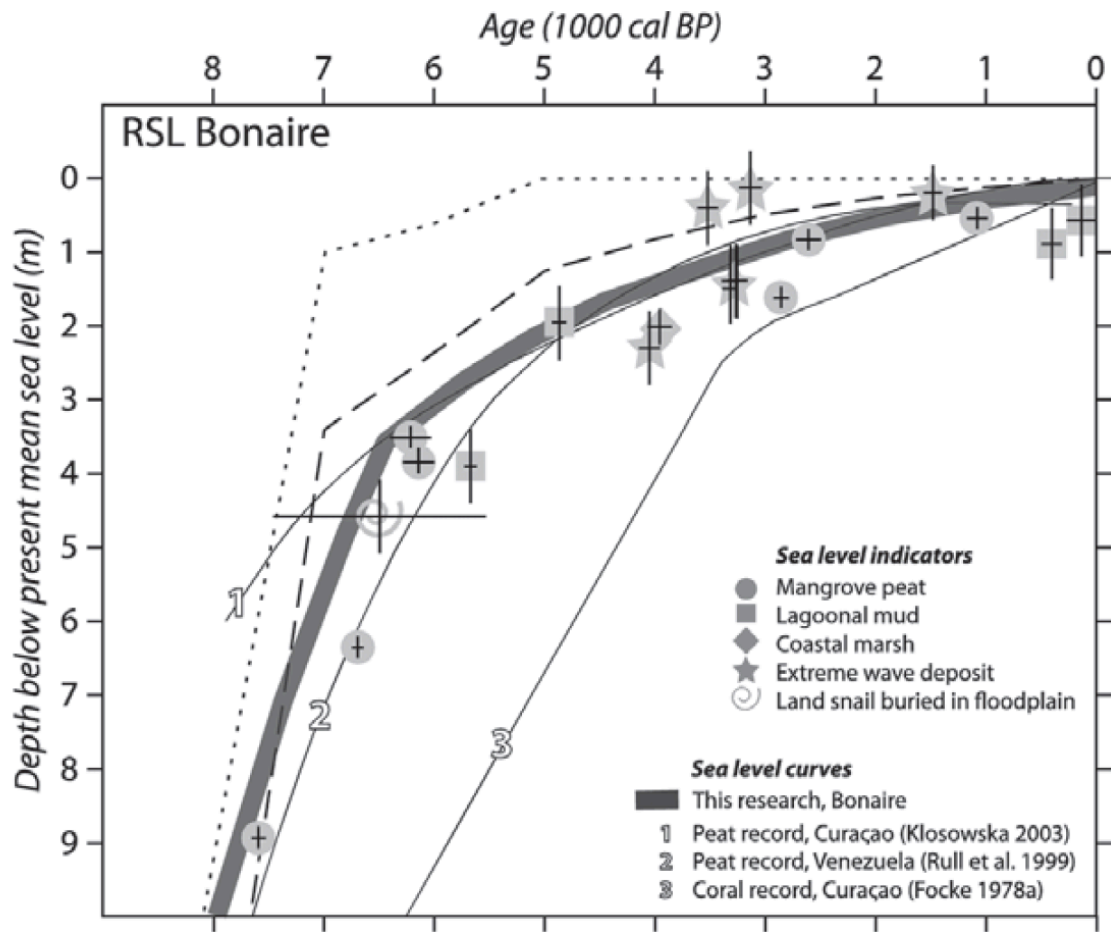


Figure 1.4: Compilation of sea level curves since the Last Glacial Maximum. The most recent update in the thick grey solid line as determined by Engel et al. (2014).

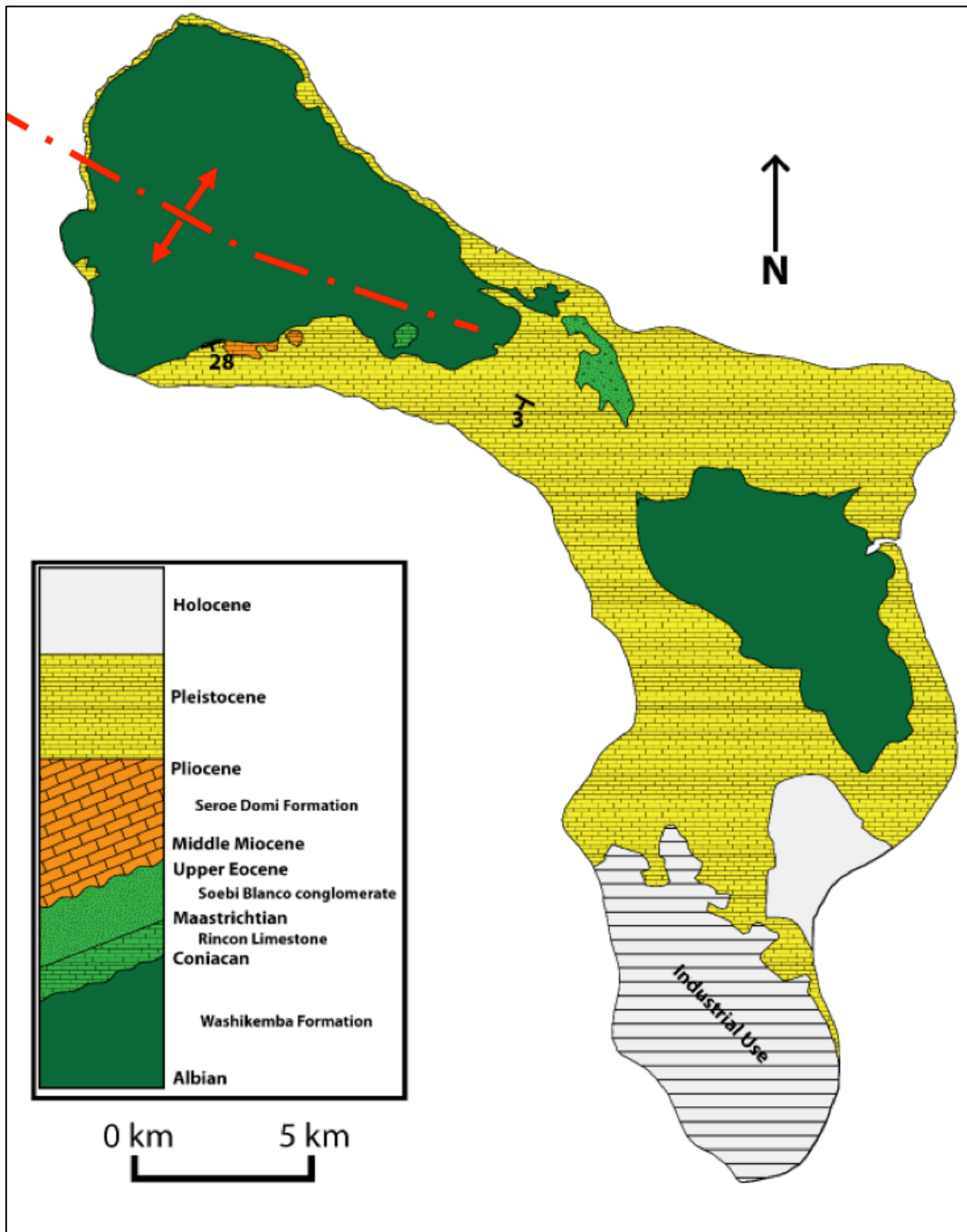


Figure 1.5: Geologic map of Bonaire with associated stratigraphic column (Sulaica, 2015) and interpreted anticline axis (Hippolyte and Mann, 2011; Silver et al., 1975).

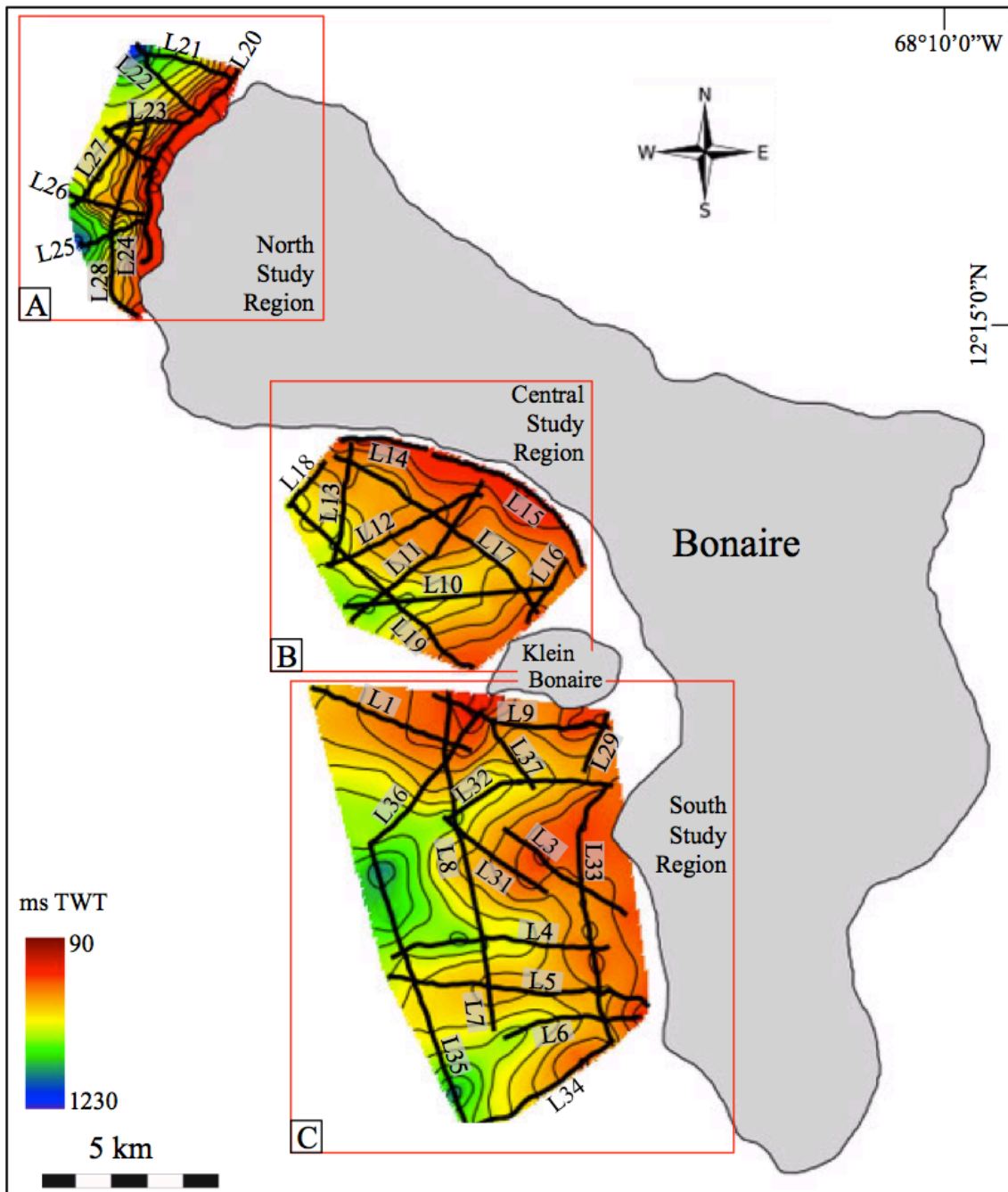


Figure 1.6: Island of Bonaire with Texas A&M University marine seismic survey profile locations and names (black lines). Red boxes (A-C) outline the three different study regions. Seismic derived seafloor bathymetry for each region contoured every 100 m.

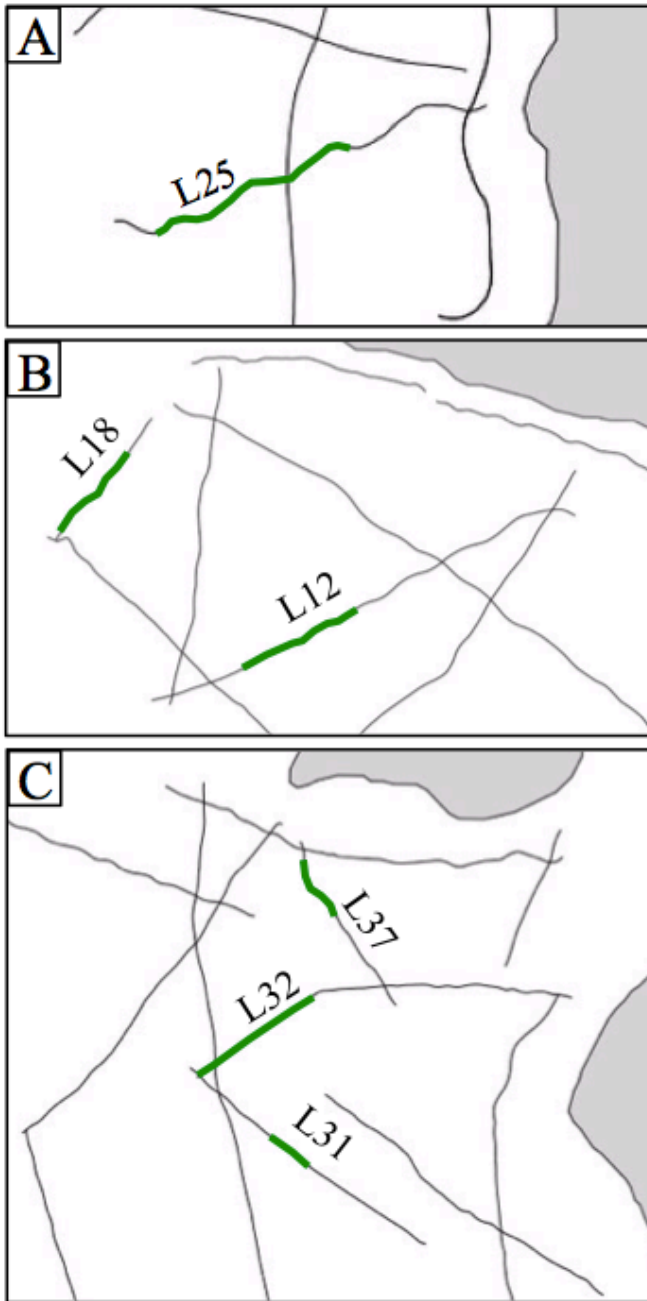


Figure 2.1: Map insets for the six seismic lines that contain sub-seafloor reflectors. Dark grey represents Bonaire coastline. Green highlights the location of the reflector on each respective line in the three regions (A) north, (B) central, (C) south. Line location shown in Fig. 1.6.

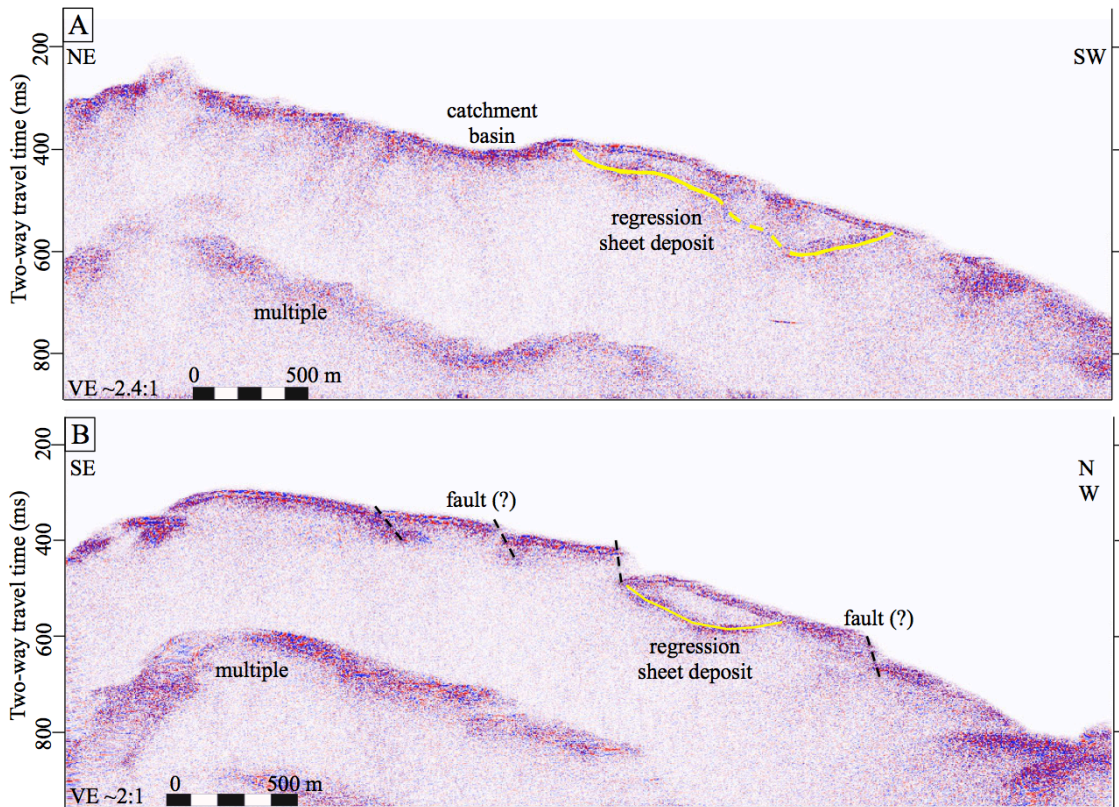


Figure 2.2: Seismic reflection profiles showing examples of the sub-seafloor reflector interpreted as the base of a regression sheet deposit (yellow lines). (A) Seismic line 12 exhibits an example of a hummocky, discontinuous reflector. (B) Seismic line 31 exhibits lens shaped feature with continuous subsurface reflector as the base. Line locations shown in Fig. 1.6.

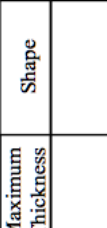
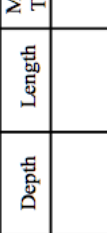

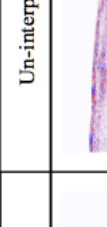
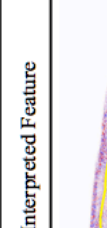
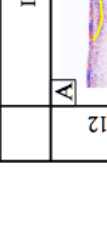


	Interpreted Feature	Un-interpreted Feature	Depth	Length	Maximum Thickness	Shape
Line 12	 A noVE		445 ms TWT	1,331 m	53 ms TWT	Hummocky
Line 18	 B 3VE		500 ms TWT	806 m	40 ms TWT	Hummocky
Line 25	 C 3VE		386 ms TWT	978 m	60 ms TWT	Hummocky
Line 31	 D noVE		485 ms TWT	485 m	42 ms TWT	Lens
Line 32	E noVE		660 ms TWT	2,031 m	60 ms TWT	Lens
Line 37	F noVE		428 ms TWT	543 m	46 ms TWT	Hummocky

Figure 2.3: Seismic reflection profiles showing sub-seafloor reflectors observed in six seismic lines. (A), (B), (C), and (F) represent hummocky shaped reflectors while (D) and (E) are lens shaped. Discontinuous (dashed yellow lines) and continuous (solid yellow lines) reflectors represent the base of a regression sheet deposit. Green solid line represents the base of a slide or slump deposit. Feature location in Fig. 2.1.

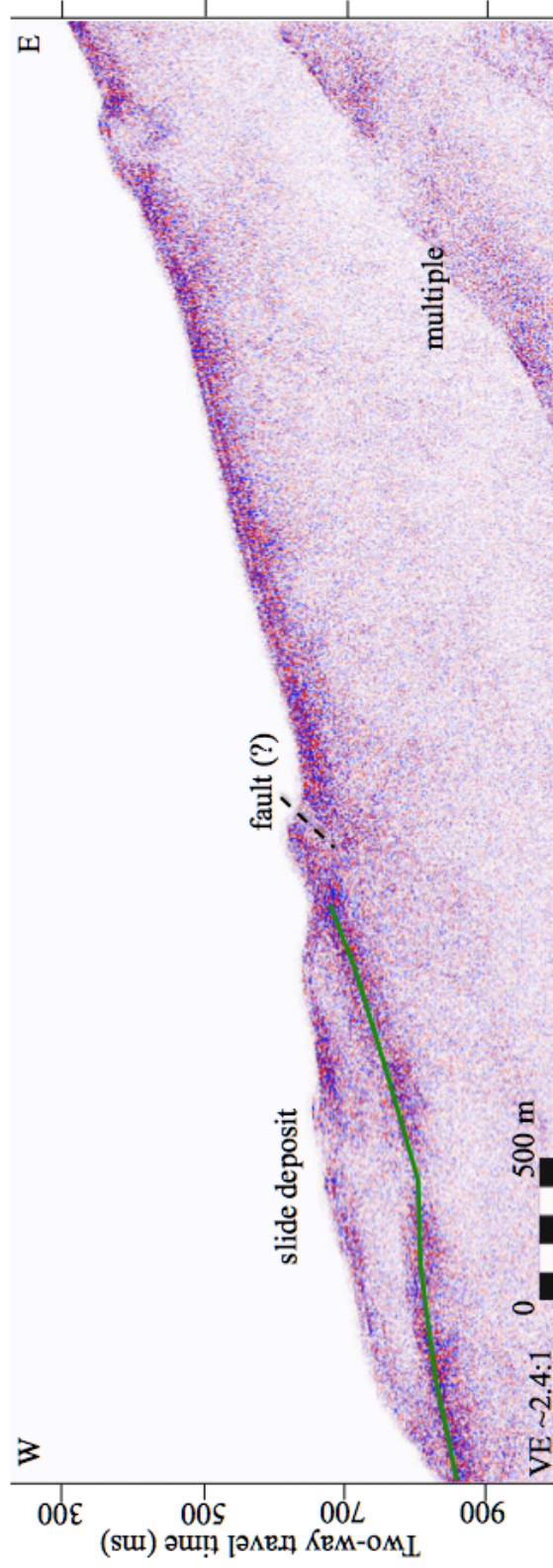


Figure 2.4: Seismic reflection profile of line 32 showing the sub-seafloor reflector (green line) interpreted to be the base of a slide deposit on the slope flank. Fault interpreted by Bayer, 2016. Line location shown in Fig. 1.6.

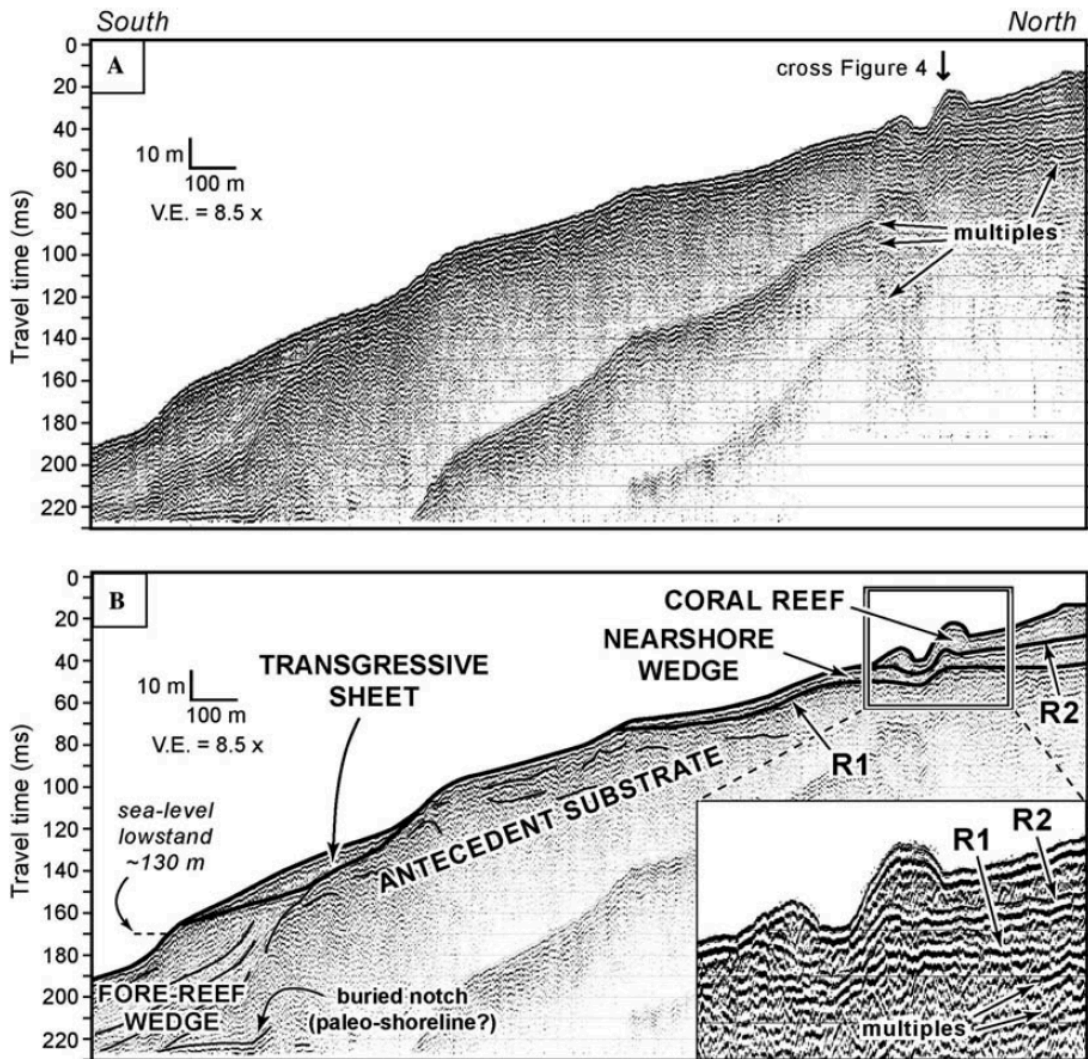


Figure 2.5: Seismic reflection image of the reef complex shelf on the leeward shore of Molokai, Hawaii. (B) Transgressive sheet interpreted on top of the antecedent substrate and inset displays modern coral reef growth (Barnhardt et al., 2005).

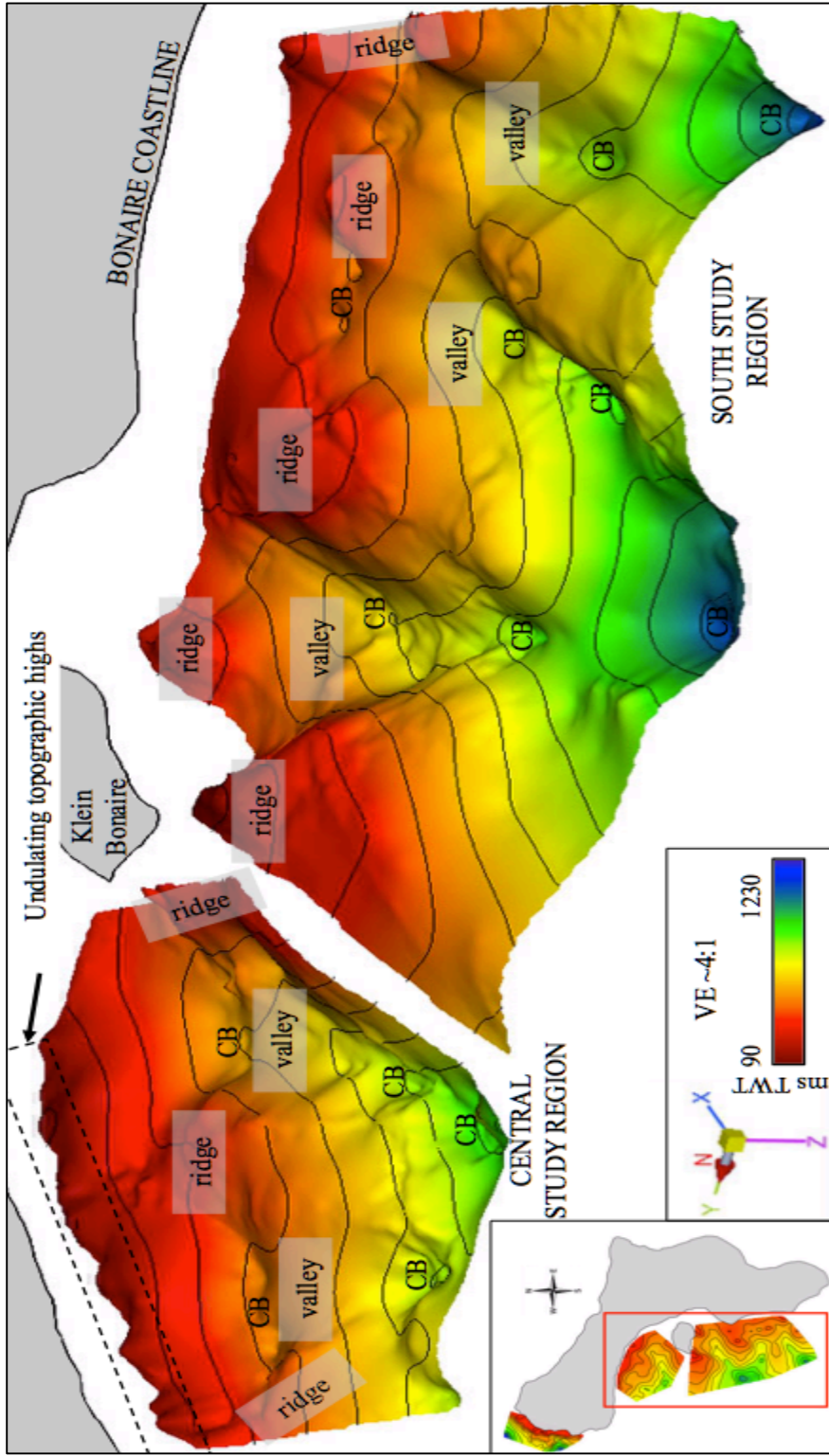


Figure 2.6: Seismic derived seafloor bathymetry for the central and south study regions contoured every 100 m. Interpretation of major topographic features labeled including ridges, valleys, catchment basins (CB), and undulating topography along the coastline in the central region (dashed box).

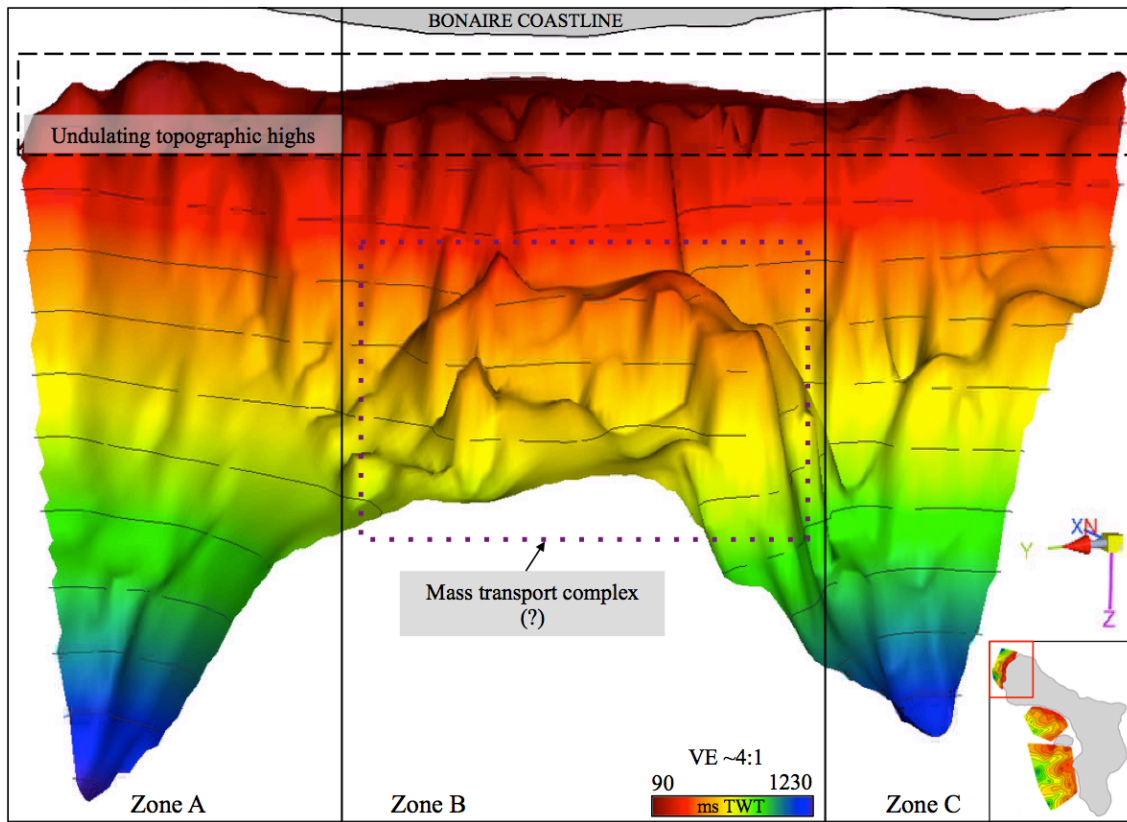


Figure 2.7: Seismic derived seafloor bathymetry for the north study regions contoured every 100 m. Possible mass transport complex in down-dip location of Zone B (dotted purple box). Undulating topographic highs along the coastline across all three zones (dashed back box).

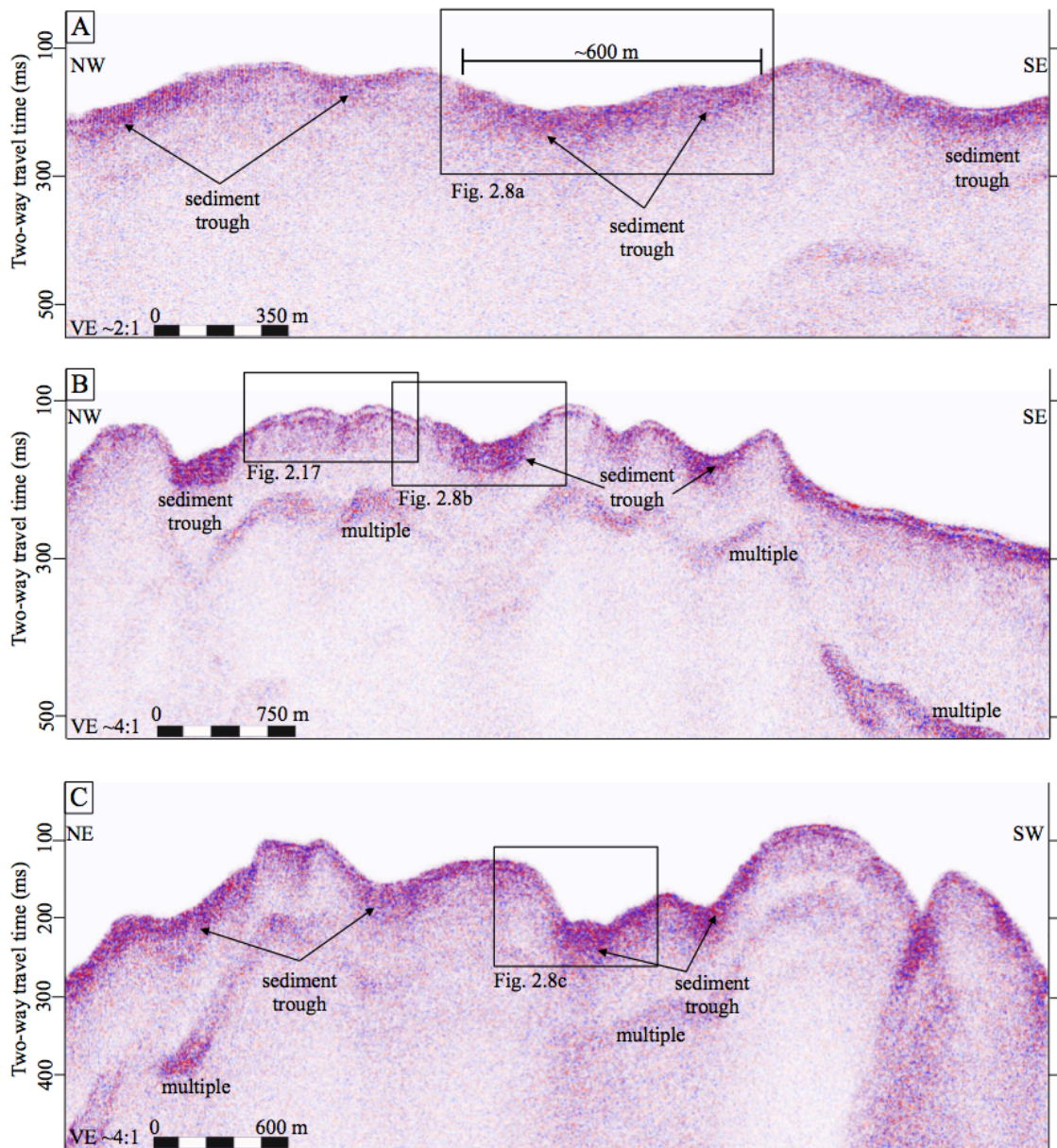


Figure 2.8: Seismic reflection profiles showing the undulating seafloor profiles along the coast in the north and central study regions (A) Line 14, (B) Line 15, (C) Line 20. Each line shows topographic lows, which are interpreted to be sediment troughs. Notice the thick, high amplitude trough surrounded by the thin, clear topographic highs. Line location shown in Fig. 1.6.

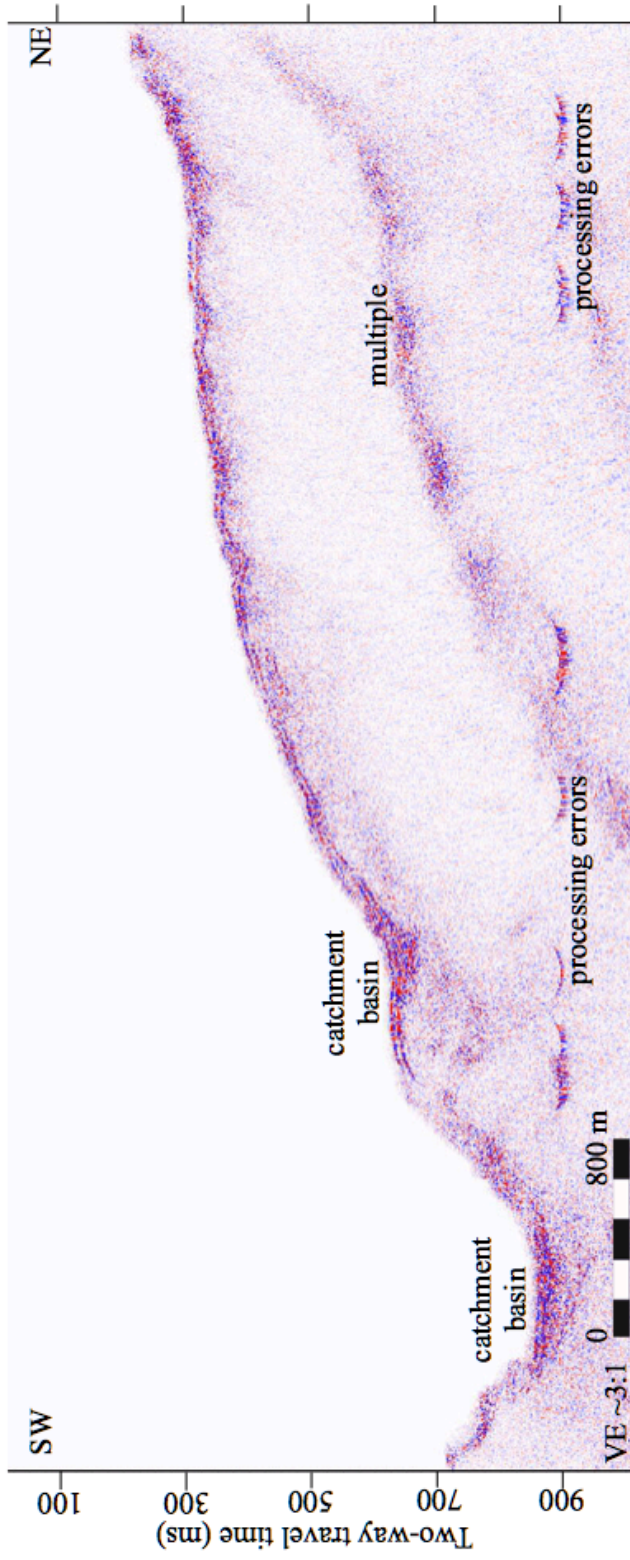


Figure 2.9: Seismic reflection line 11 down a valley in the central region showing sediment catchment basins within the valley. Notice the thick, high amplitude troughs within the local topographic lows. Line location shown in Fig. 1.6.

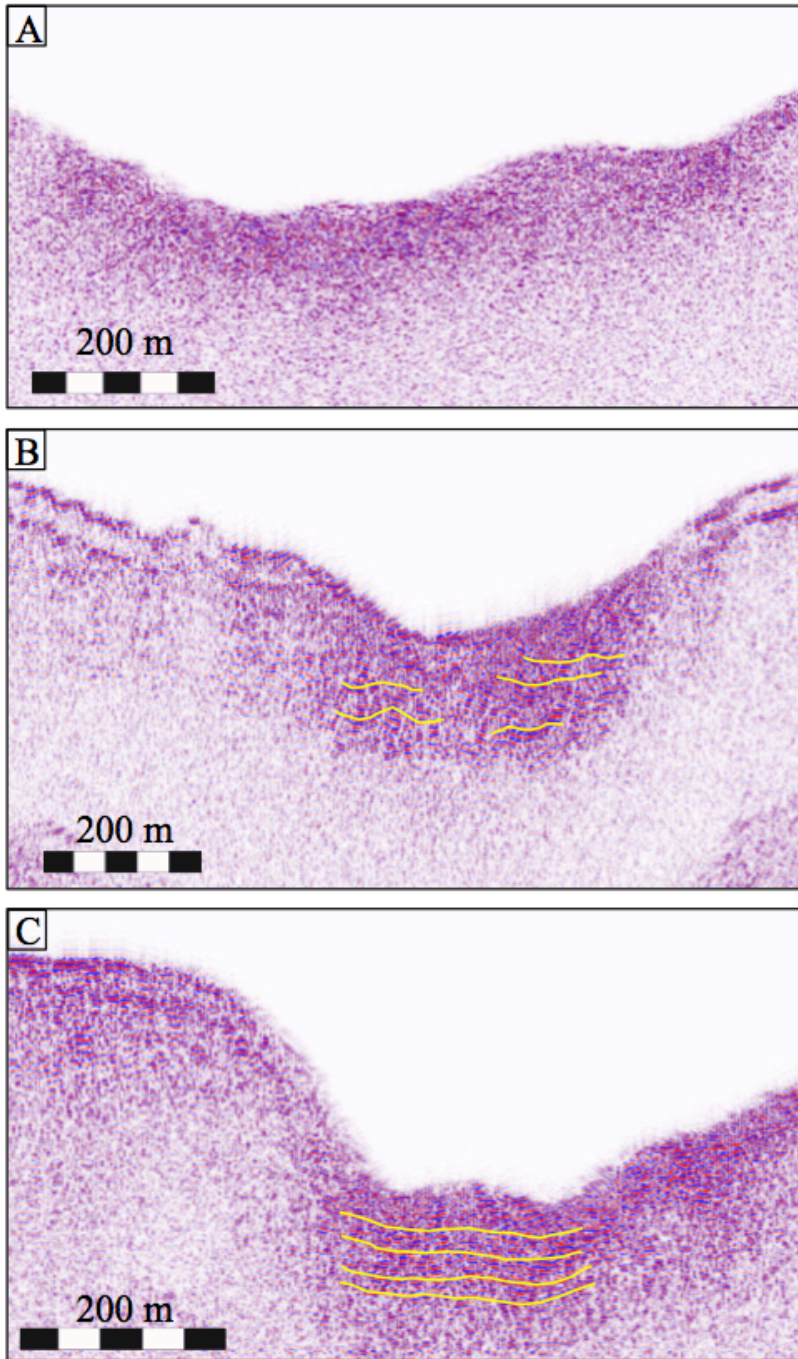


Figure 2.10: Inset images from seismic reflection profiles in Fig. 2.6 showing sediment filled troughs. (A) Line 14, (B) Line 15, (C) Line 20. Notice the thick, high amplitude trough surrounded by the thin, clear topographic highs. (A) Chaotic and discontinuous sediment reflectors. (B) and (C) semi continuous to continuous sediment reflectors.

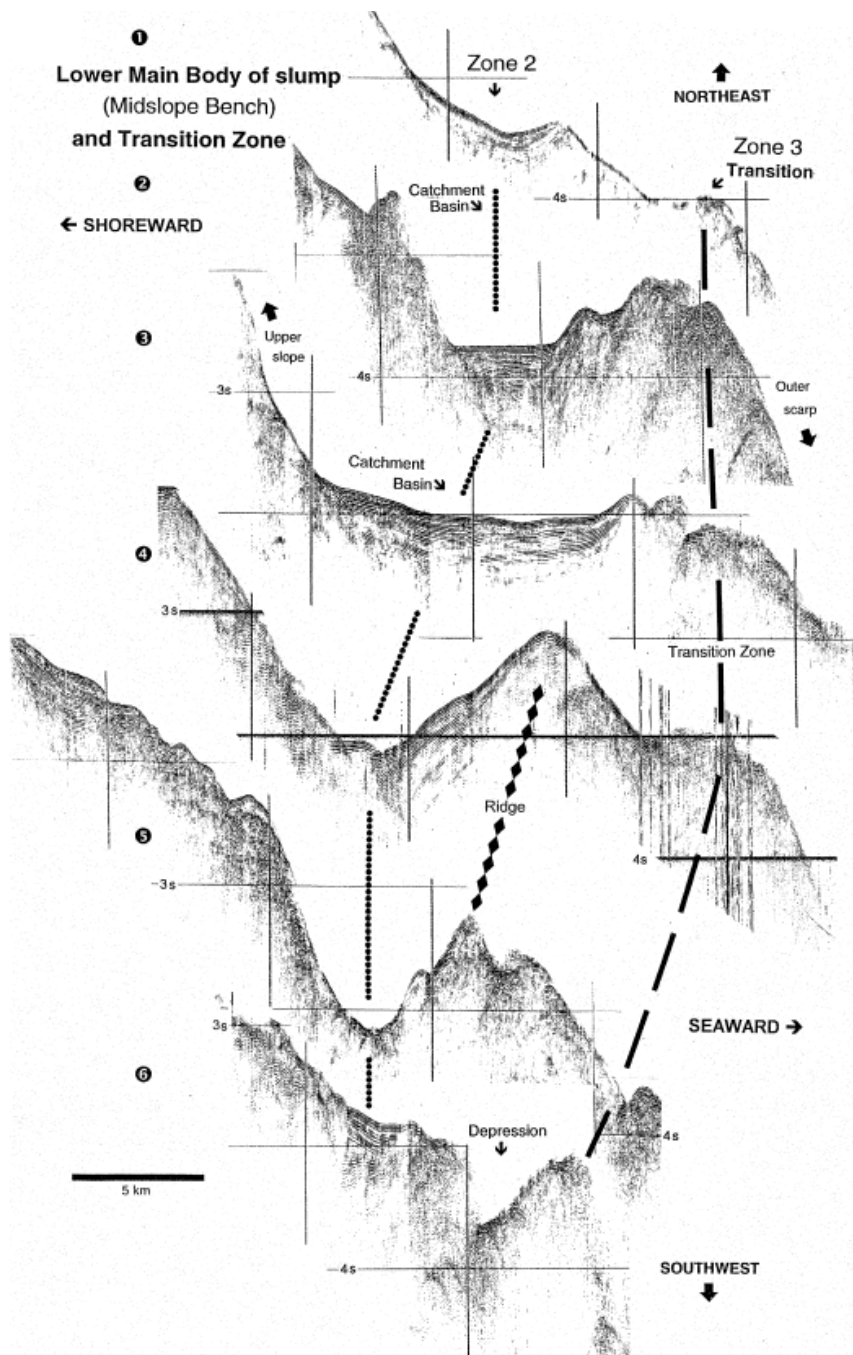


Figure 2.11: Single channel seismic reflection profiles off the oceanic volcano, Kilauea, in Hawaii. Catchment basins vary in size throughout the profiles and show seismic evidence of sediment accumulation (Smith et al., 1999).

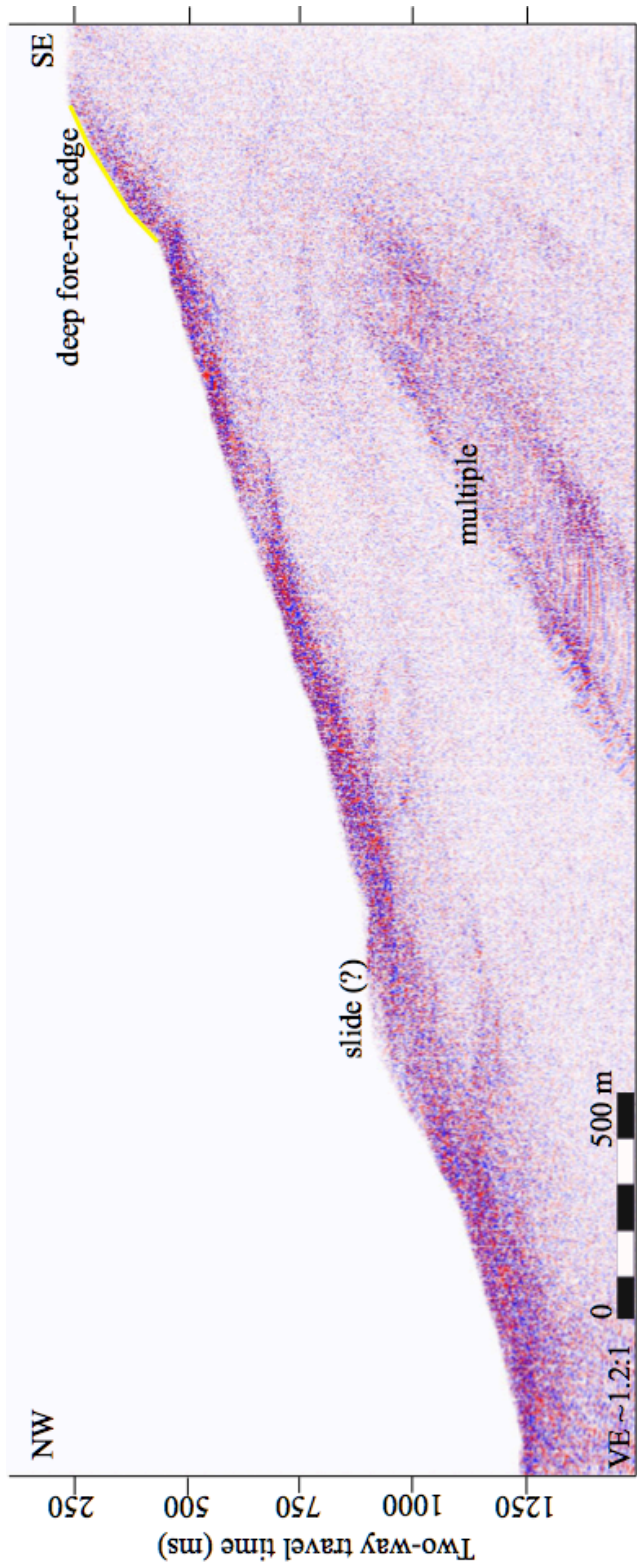


Figure 2.12: Seismic reflection profile of line 22 showing a hump-like feature (yellow line) interpreted to be the deep fore-reef edge followed by the steep, basin-ward dipping slope. Possible debris slide interpreted at the change in topography ~900 ms. Line location shown in Fig. 1.6.

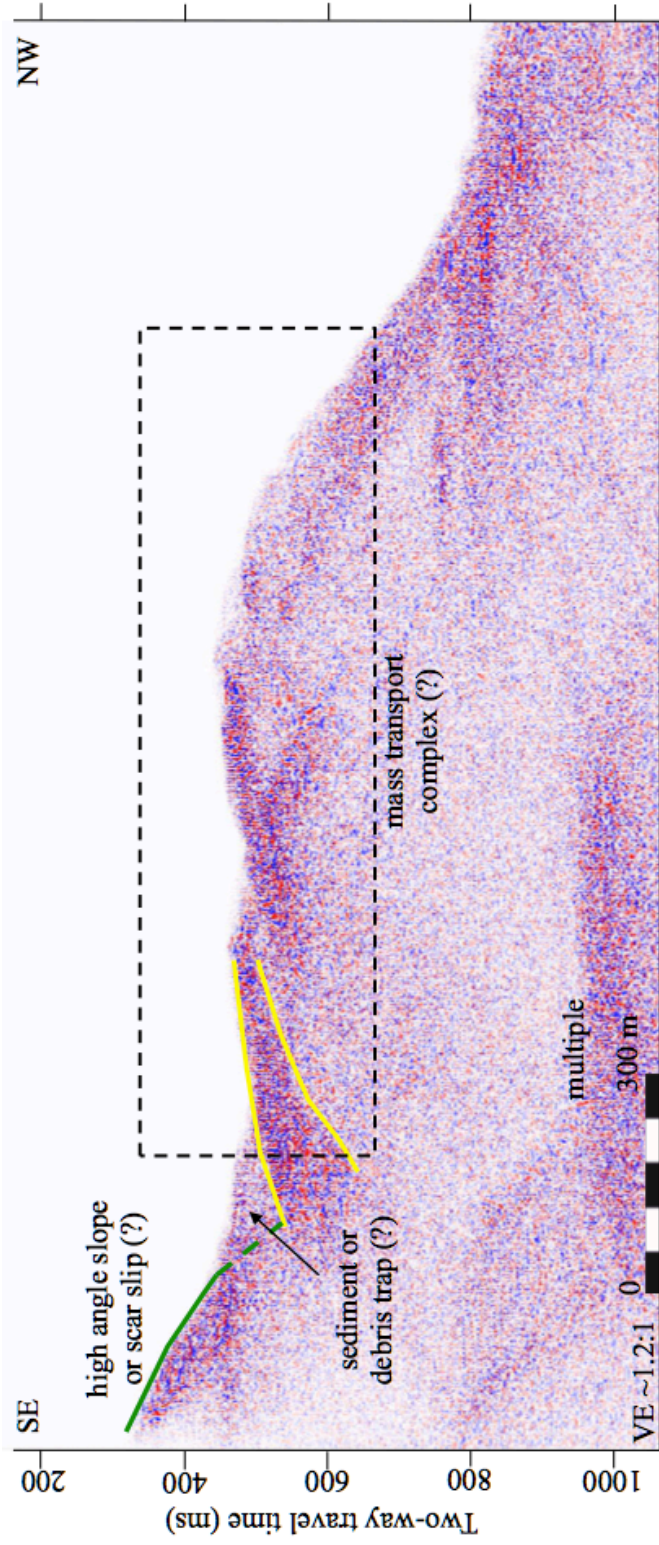


Figure 2.13: Seismic reflection profile of line 26 showing steep, basin-ward dipping slope (green line) followed by sediment or debris trap before a large topographic high theorized to be a mass transport complex. Wedge of chaotic, thick amplitude reflectors (yellow lines) at slope base, thin toward the mass transport complex (black dashed line). Line location shown in Fig. 1.6.

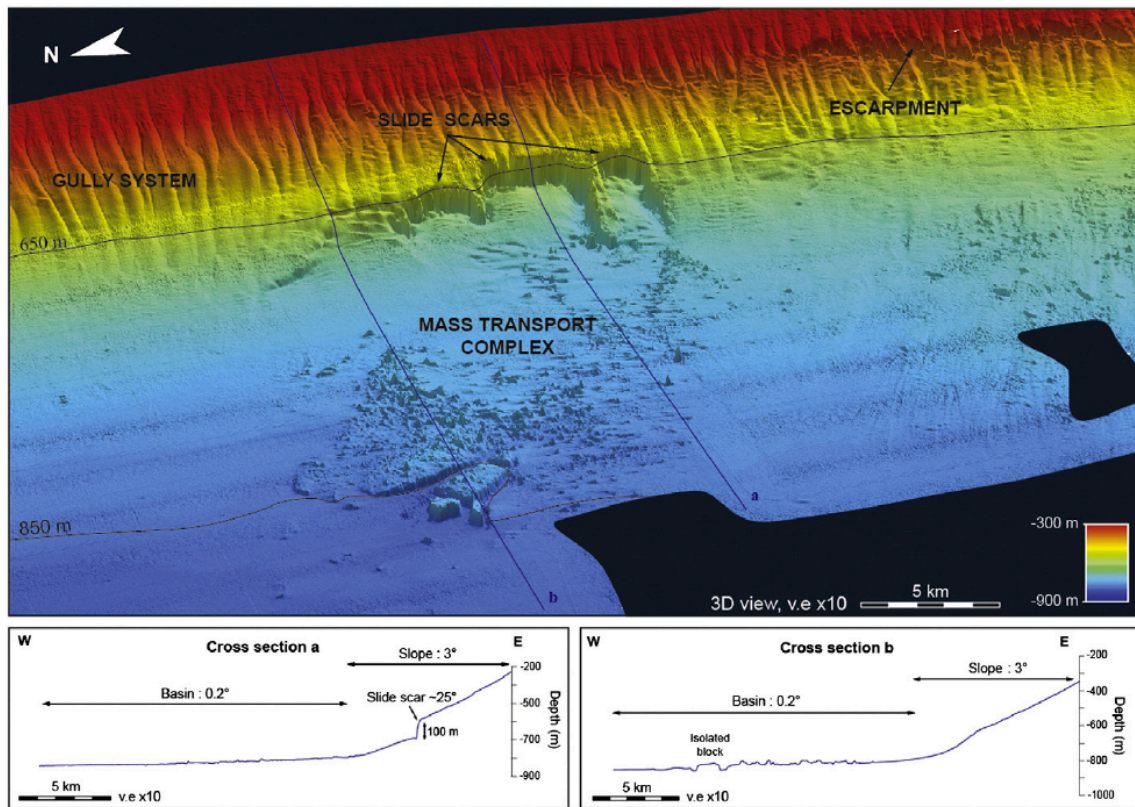


Figure 2.14: Bathymetry and cross section views of mass transport processes of large carbonate mounds due to slope failure and gravity-flow deposits along the northwestern margin of the Great Bahama Bank (Principaud et al., 2015).


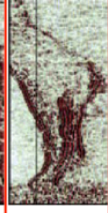
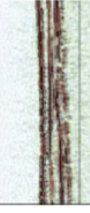
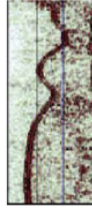
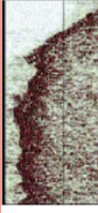
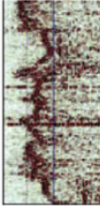

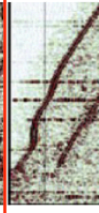
Facies	Abbreviation	Upper boundary/sea-bottom reflector	Surface gradient	Internal configuration	Lower boundary	External forms	Example
Aprons	A	Strong and continuous, attenuated when overlain by other deposits.	High-moderate near the reefs and low towards the platform/terraces.	Attenuated, divergent internal reflectors. Downlap on subparallel reflectors of L or M facies.	Continuous, strong or weak reflectors downlapping onto R, M or L facies.	Thick longitudinal wedges on the backreef, often stacked. Wedges also on the forereef and under reefs of the terrace.	
Channel deposits	Ch	Often strong and continuous.	Very high at flanks of inter-reef channels. Low at channel base. Aspect ratios vary with location.	Sub-parallel or divergent, attenuated, continuous reflectors, thickening laterally. Downlap onto base, onlap on rR and channel flanks.	Often strong, continuous. Signal generally attenuated and poor-to chaotic under the channel base.	Channelized geometry on interreef and terraces. Tend to develop levees at the outer-platform.	
Lagoon	L	Strong and continuous reflector. In some distal areas the top reflector is scattered or attenuated but continuous.	Low.	Alternating attenuated and strong sub-parallel reflectors. May onlap on R.	Usually a strong continuous reflector interrupted by irregular patterns that suggest erosion.	Continuous sheet drape, interrupted by R or by pinch-out against underlying reflectors.	
Mounds	M	Strong and continuous, wavy.	Low at the top, moderate-to-high at the flanks.	Internal reflectors attenuated but visible. Either subparallel to seabottom or oblique, downlapping against L or other M facies.	Blurry on top of R facies, or flat, often strong, poorly-continuous to continuous on top of L facies.	Partly-connected network of mounds and depressions, abundant on the terrace or on the inner-platform.	
Reefs	br	Strong reflector moderately scattered by the presence of pinnacles or by the modern reef surface.	Very high on the flanks, low on internal terraces and notches.	Attenuated chaotic internal reflectors, except for rare flat reflectors of poor lateral extension.	No lower boundary clearly distinguished.	Elongated, prominent banks cut by inter-reef channels. Reflectors of L or A facies onlap at the flanks.	
Distal reefs	dR	Spiky strong reflectors sometimes highly attenuated and/or scattered, transition laterally to mound facies.	Low to moderate.	Internal reflections are rather chaotic except for few oblique, poorly-continuous reflectors.	Lower boundary seldom distinguished. Some lines underlain by flat continuous reflectors.	Linear, non-prominent, long reef banks, with an irregular and spiky upper boundary.	
Relict reefs	rR	Strong or significantly attenuated when not exposed in the seabottom, continuous.	Varied.	Internal reflectors are generally very attenuated and poorly recognized.	When distinguished, generally flat, continuous reflectors.	Isolated pinnacles or ridges of limited extension. Often covered by onlapping continuous reflectors.	
Slope deposits	S	Strong and continuous.	High to moderate.	Attenuated reflectors, subparallel to divergent, terminate near the forereef. Basal downlap and onlap.	Continuous strong reflector fading downdip.	NW-SE wedge with lenticular dip cross-section thickening at the forereef slope, thinning towards the basin.	

Figure 2.15: Facies descriptions from 2D seismic lines collected at the continental shelf edge in the south central Great Barrier Reef (Hinestroza et al., 2014). Channel deposits (a), reefs (b), and slope deposits (c) show similar seismic characteristics to features observed in the Texas A&M marine seismic survey.

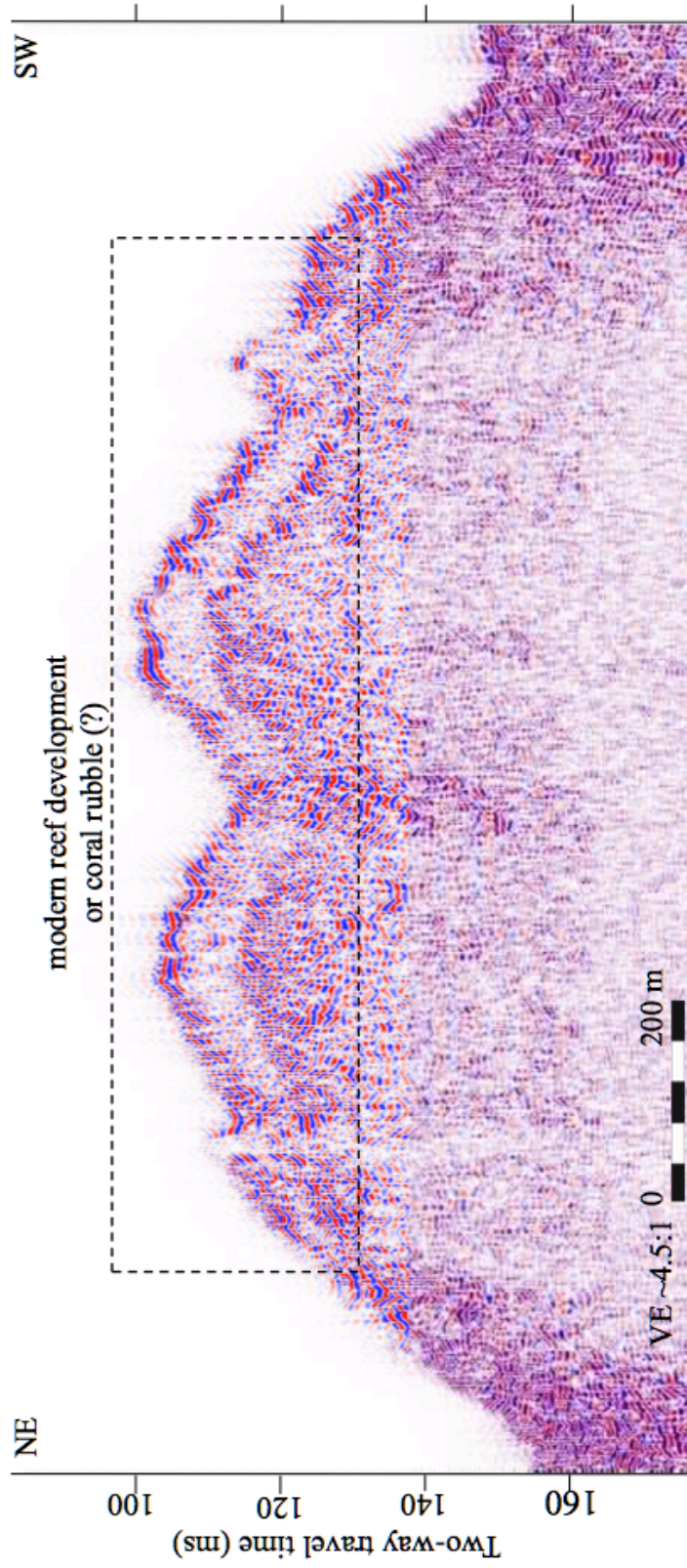


Figure 2.16: Inset image from Fig. 2.5b of seismic line 15 showing one region within the dataset where the seafloor had potentially to be subaerially exposed during the LGM. Notice the highly irregular seafloor atop of the topographic high that is interpreted as modern reef development or coral rubble (black dashed box).

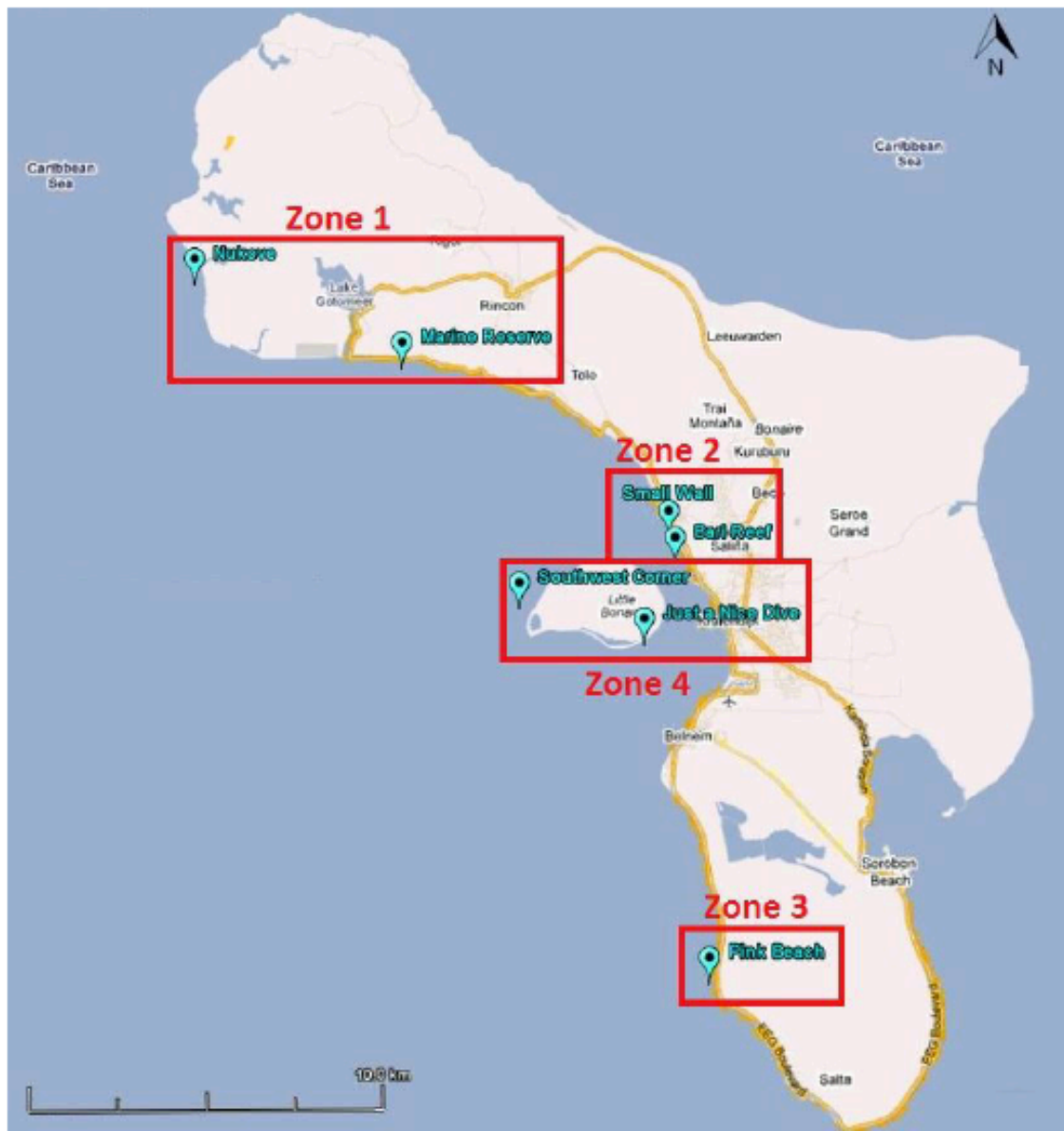


Figure 2.17: Four data collection zone locations that contain bathymetry, backscatter, and still images used to make observations in near shore locations and confirm interpretations from the marine seismic profiles (Keller 2011).

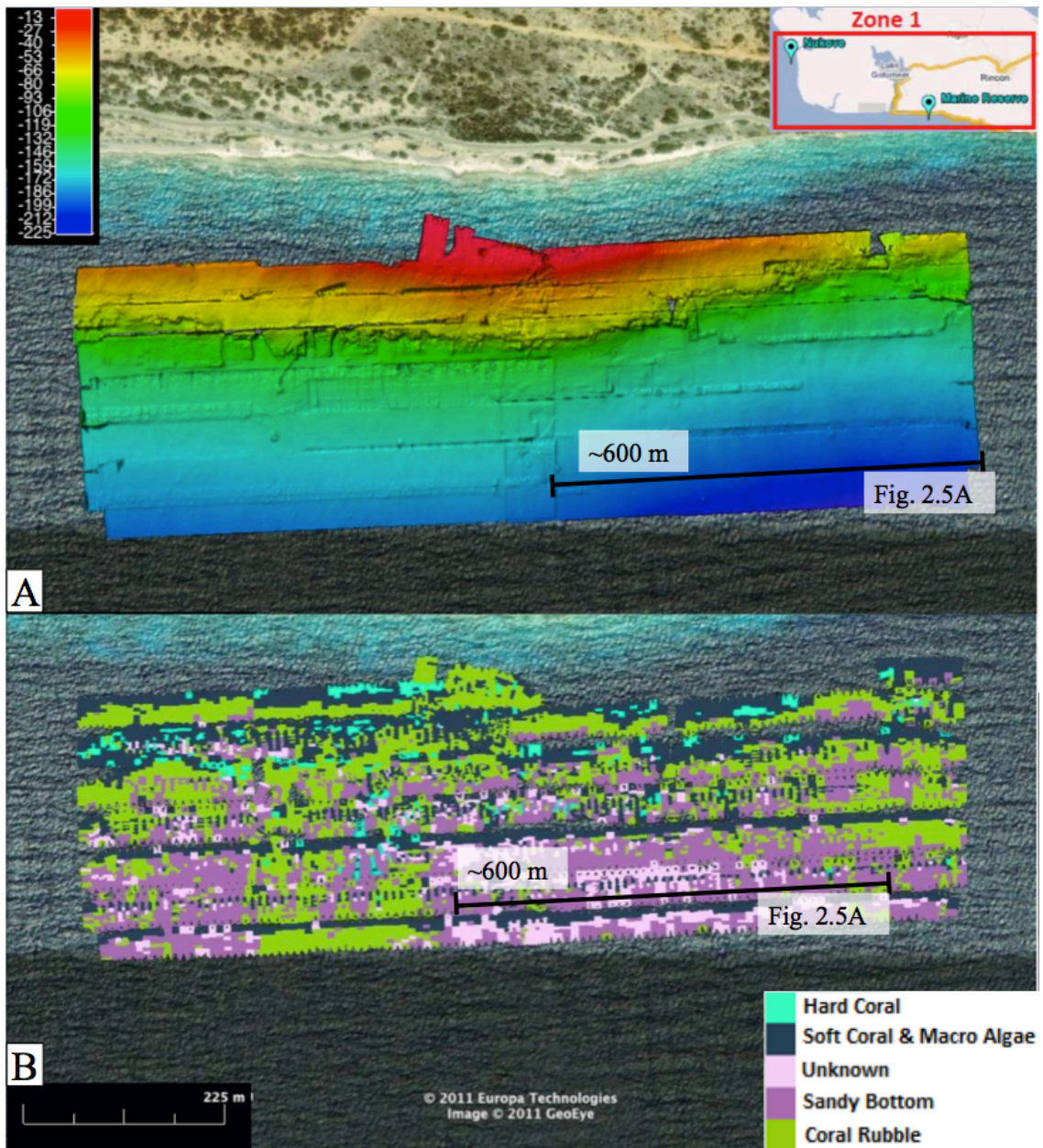


Figure 2.18: (A) Bathymetry and (B) classification map of the Marine Reserve location in Zone 1. Black transect over dark purple, sandy bottom, and dark blue, depths $\sim >200$ m corresponds to the sediment filled trough in figure 2.6. Modified from Keller (2011).

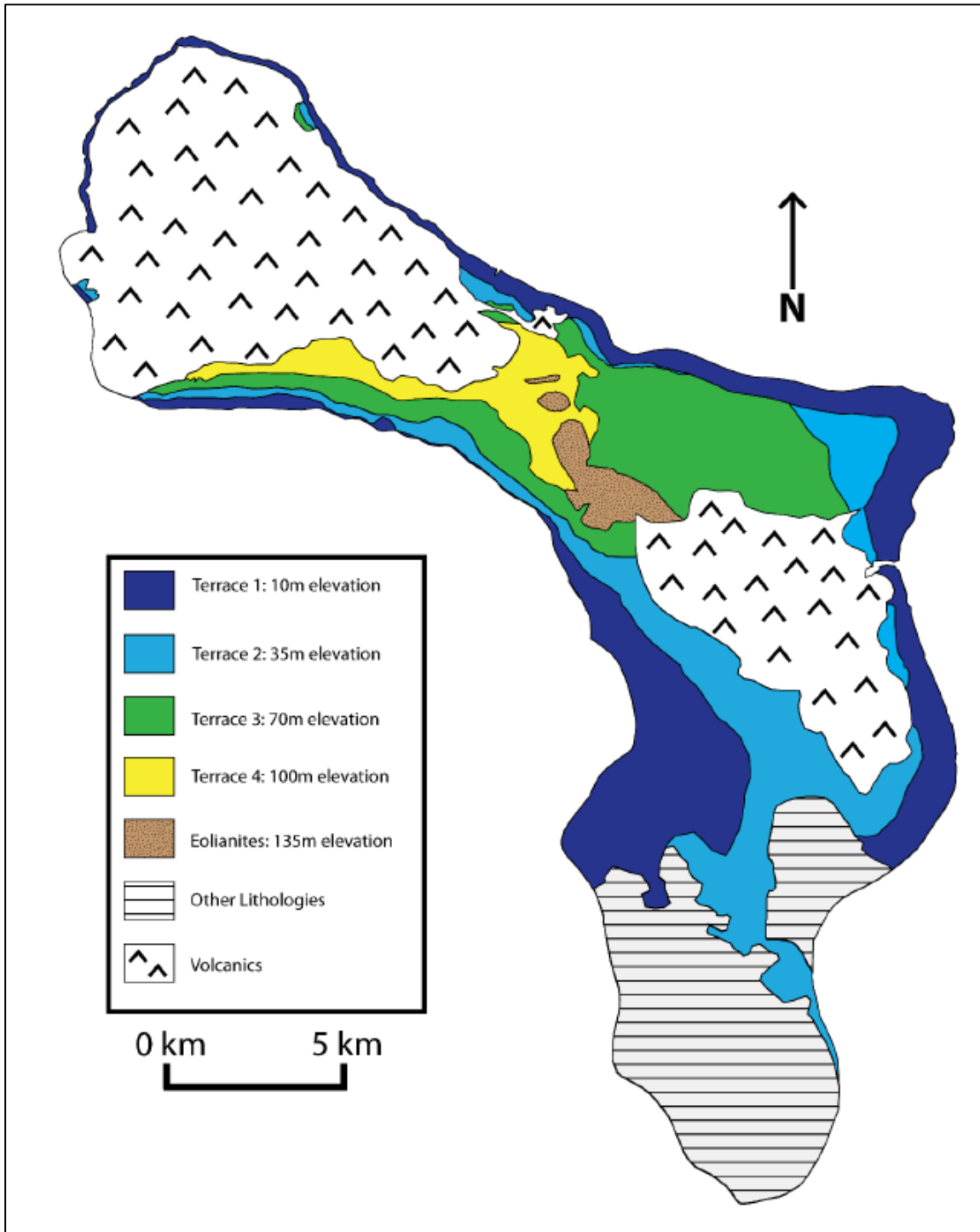


Figure 3.1: Map of Bonaire illustrating the extent of the four terraces outcropped on land (Sulaica, 2015).

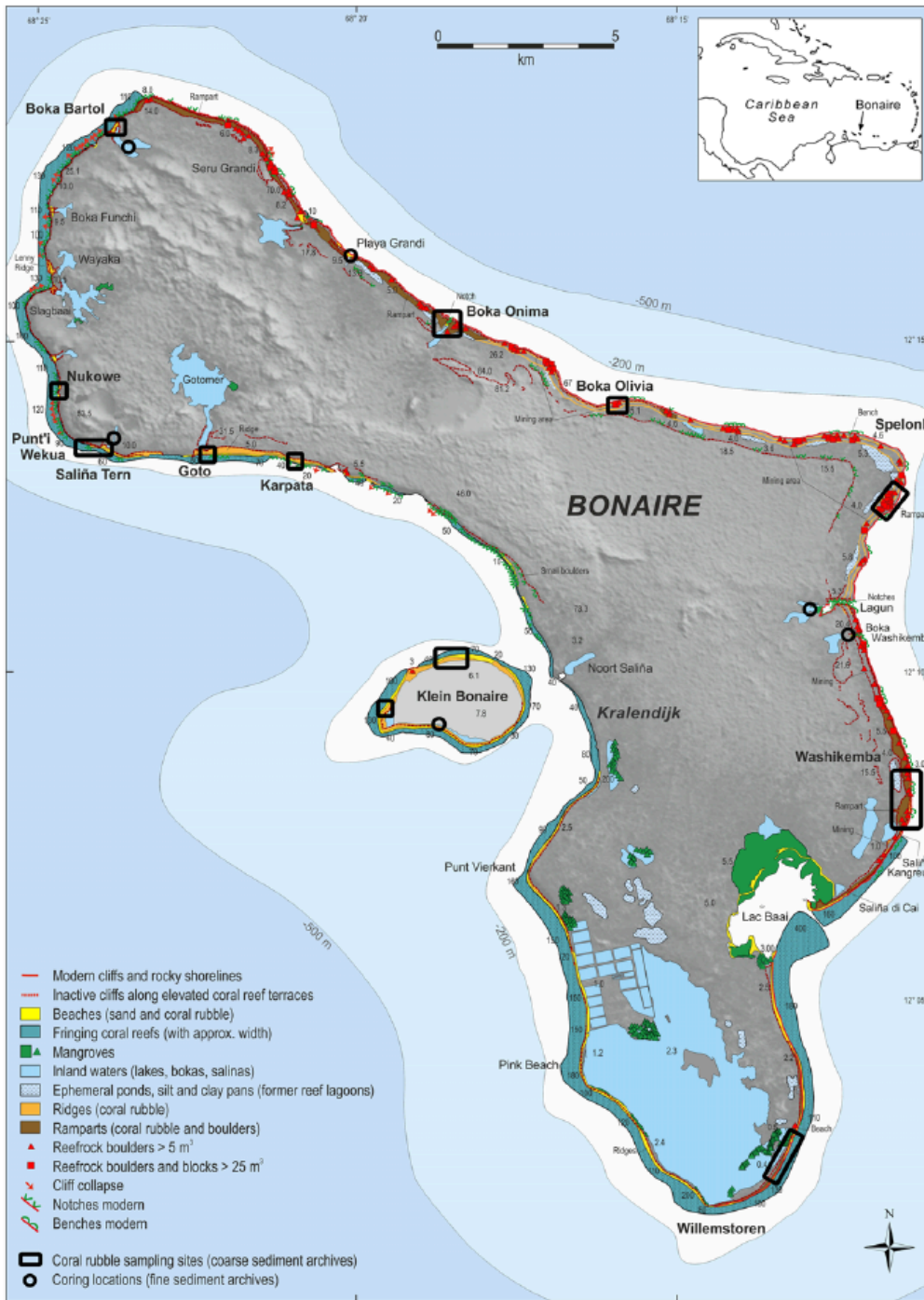


Figure 3.2: Compilation of geologic studies of the coastal morphology and coastal environments around Bonaire and Klein Bonaire (Scheffers et al., 2013). Notice the vague bathymetry contours at 200 and 500 m that were interpreted, by the authors, using aerial photographs.

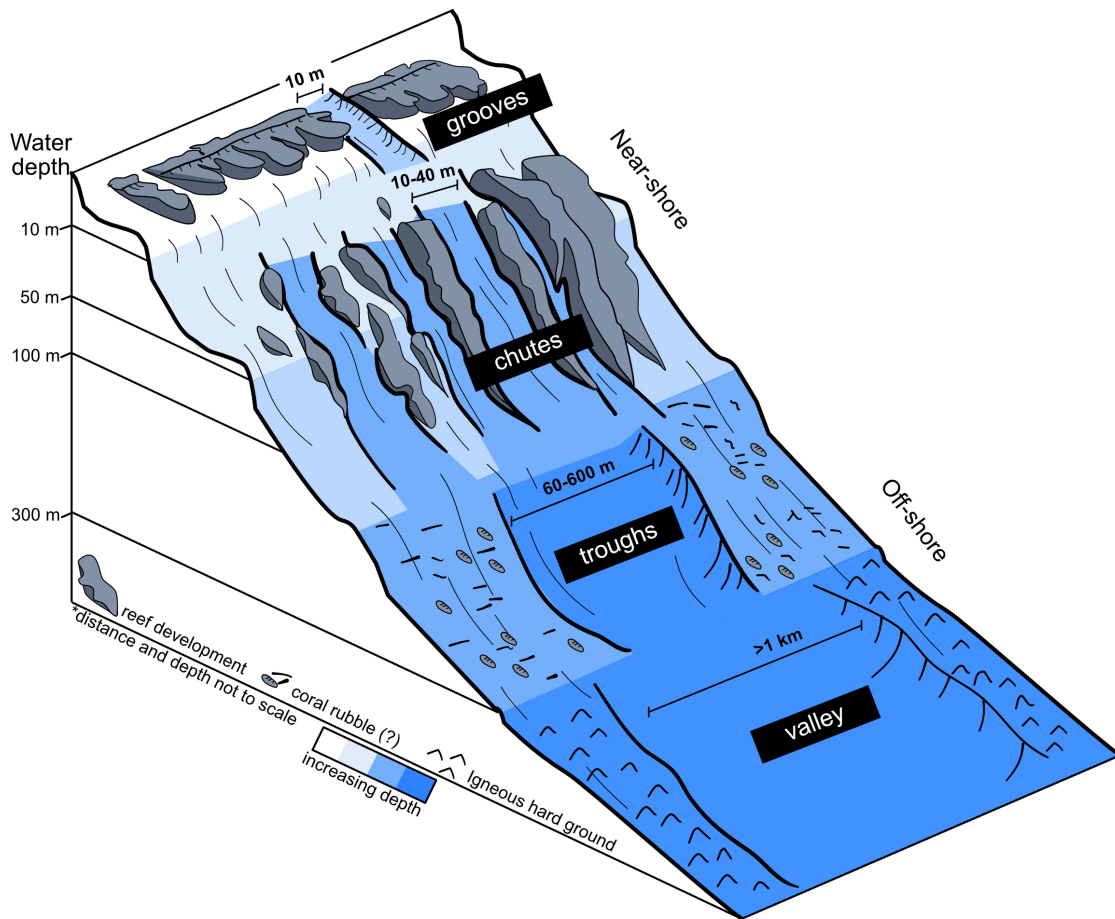


Figure 3.3: Schematic diagram of the four-stage sediment pathways off the coast of Bonaire. From the near-shore environment where sediment moves through grooves and chutes, widening to the offshore environment where sediment is transported through troughs and valleys. Image not to scale.